3D Biofabrication Strategies for Tissue Engineering and Regenerative Medicine

Piyush Bajaj,[1,2,4,*] Ryan M. Schweller,[5,*] Ali Khademhosseini,[6,7,8,9,10] Jennifer L. West,[5] and Rashid Bashir[1,2,3]

[1]Department of Bioengineering, [2]Micro and Nanotechnology Laboratory, [3]Department of Electrical and Computer Engineering, University of Illinois Urbana-Champaign, Urbana, Illinois 61801; email: rbashir@illinois.edu

[4]Defense System and Analysis Division, Los Alamos National Laboratory, Los Alamos, New Mexico 87545

[5]Department of Biomedical Engineering, Duke University, Durham, North Carolina 27708

[6]Center for Biomedical Engineering, Department of Medicine, Brigham and Women's Hospital, Harvard Medical School, Cambridge, Massachusetts 02139

[7]Wyss Institute for Biologically Inspired Engineering, Harvard University, Boston, Massachusetts 02115

[8]Harvard-MIT Division of Health Sciences and Technology, Massachusetts Institute of Technology, Cambridge, Massachusetts 02139

[9]Department of Maxillofacial Biomedical Engineering and Institute of Oral Biology, School of Dentistry, Kyung Hee University, Seoul 130-701, Republic of Korea

[10]Department of Physics, King Abdulaziz University, Jeddah 21569, Saudi Arabia

Annu. Rev. Biomed. Eng. 2014. 16:247–76

First published online as a Review in Advance on May 29, 2014

The *Annual Review of Biomedical Engineering* is online at bioeng.annualreviews.org

This article's doi: 10.1146/annurev-bioeng-071813-105155

*Equal contribution

Keywords

hydrogels, stem cells, scaffolds, bioprinting, photolithography, vascularization

Abstract

Over the past several decades, there has been an ever-increasing demand for organ transplants. However, there is a severe shortage of donor organs, and as a result of the increasing demand, the gap between supply and demand continues to widen. A potential solution to this problem is to grow or fabricate organs using biomaterial scaffolds and a person's own cells. Although the realization of this solution has been limited, the development of new biofabrication approaches has made it more realistic. This review provides an overview of natural and synthetic biomaterials that have been used for organ/tissue development. It then discusses past and current biofabrication techniques, with a brief explanation of the state of the art. Finally, the review highlights the need for combining vascularization strategies with current biofabrication techniques. Given the multitude of applications of biofabrication technologies, from organ/tissue development to drug discovery/screening to development of complex in vitro models of human diseases, these manufacturing technologies can have a significant impact on the future of medicine and health care.

Contents

1. INTRODUCTION

The current waiting list for organ transplant recipients has grown steadily in the past few decades to over 120,000 candidates (>75,000 are active[1]) in the United States alone (as of March 2014; see United Network of Organ Sharing, **http://www.unos.org**). There is a huge crisis in meeting this additional demand, and the gap continues to widen (**Figure 1**). Currently, the transplantation of vital organs such as kidney, liver, heart, and lung is the only treatment for their end-stage failure. Every day, about 79 people receive some type of organ transplant. However, each day an average of another 18 people die waiting for an organ transplant because of supply shortages (1). To close this transplantation gap, tissue engineering and regenerative medicine approaches offer the promise of new or restored tissues and organs through the combination of material scaffolds and a patient's own cells (2, 3). Although past work has generated methods to create artificial skin (4), cartilage (5), tracheas (6), and bladders (7), these represent relatively simple structures compared with the complex architectures of heterogeneous or vascularized organs and tissues (8). As a result, the promise of new or restored tissues and organs through engineering has been left largely unrealized. **Figure 2** shows an overview of the tissue engineering–based approach for de novo organogenesis.

Recent advances in tissue engineering owe their success largely to the development of novel biomaterials-based strategies that better mimic native tissue and organ structures. These biomaterials are capable of harnessing the innate abilities of cells to sense their local environment through cell–cell and cell–extracellular matrix (ECM) contacts and self-assemble into complex networks to elucidate emergent behaviors. Many past studies have focused on tuning the bulk properties (i.e., biomolecule concentrations, mechanical properties) of these materials, which assumes that the native cellular environment is homogeneous across multiple length scales. Although modern biomaterials permit the investigation of complex cellular behaviors such as mouse mesenchymal stem cell (mMSC) differentiation (9) and epithelial-mesenchymal transition (EMT) of adenocarcinomas (10), they have yet to accurately replicate the heterogeneous nature of native cellular environments. Much of this is due to the inherent difficulty of precisely tailoring three-dimensional (3D) environments. Although many intricate methods have been developed to generate complex two-dimensional (2D) patterns and gradients of biochemical and mechanical cues, 2D culture conditions may not be appropriate for many cell types (11–13). Furthermore, 2D fabrication techniques often cannot be readily translated into 3D culture systems. Therefore,

[1]An active candidate is considered eligible for an organ transplant at a given point in time. Some candidates are inactive, as they are considered medically unsuitable for a transplant or need to fulfill some additional eligibility requirement(s).

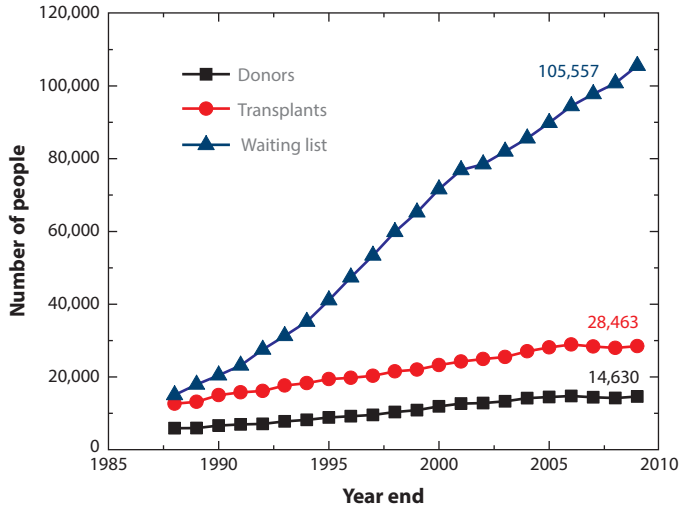

Figure 1

The gap between the number of people waiting for an organ transplant and the number of people receiving one continues to widen. (Data obtained from 1).

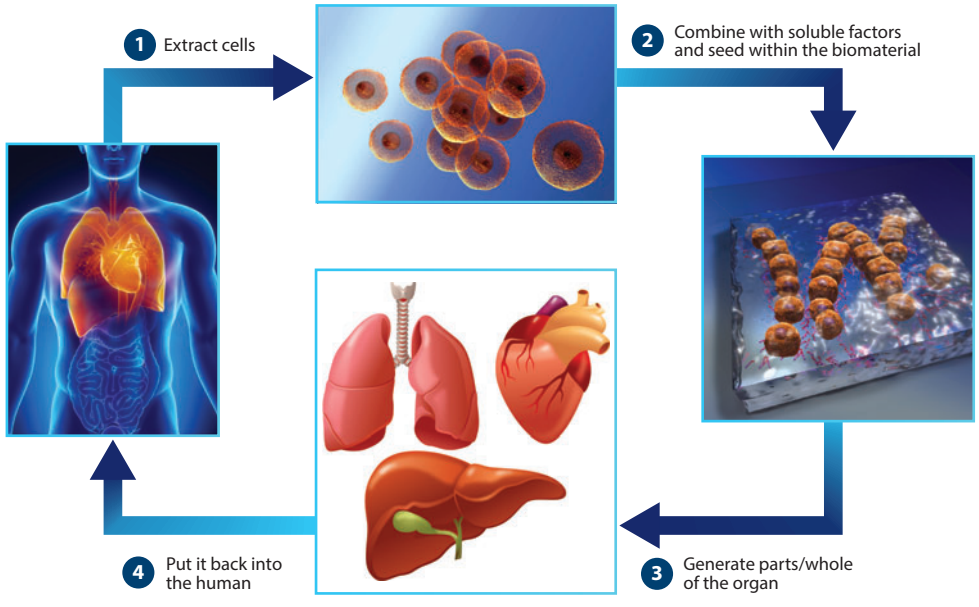

Figure 2

Overview of the tissue engineering–based approach using three-dimensional (3D) biofabrication for de novo organogenesis.

there is a need to adapt these 2D methods and/or create entirely new methods to accurately capture the complex 3D cellular environment.

Recently, several methods have been developed to spatially encode local properties to 3D materials-based culture systems, and we generically refer to these methods as 3D biofabrication techniques. Such methods are capable of either constructing or patterning materials, with a high degree of control, by finely tuning and defining material geometries, localization of biomolecular cues, and/or mechanical properties. In doing so, they have created complex material geometries to resemble endogenous tissues (14). Similarly, biofabrication-based patterning techniques have immobilized controlled concentrations of adhesive ligands, growth factors, or other signaling molecules to mimic cellular architectures in vivo (15). By enabling this precise control over local and bulk material properties, these methods can create new biomaterials that better replicate the complex and heterogeneous nature of endogenous tissues and organs. This will help to bridge the gap between the current state of tissue engineering and the unrealized hope of true artificial organs and tissues. In addition, this level of control could allow for a more complete model of cancerous or disease states in cells and tissues to assess current, or develop new, therapeutic strategies. In this review, we discuss various biomaterial properties and how different 3D biofabrication strategies can be used to create complex 3D cellular environments using biomaterials.

2. MATERIALS AS SCAFFOLDS FOR TISSUE ENGINEERING

Owing to the wide spectrum of mechanical and biochemical properties of native tissue, a variety of materials have been developed to mimic specific cell and tissue niches (16). Hydrogels are the most commonly explored materials for fabricating the complex 3D cellular microenvironments, as they can be tuned for ideal degradability and mechanics and the ability to incorporate biomolecules of interest. They are generally considered to have high biocompatibility and nonimmunogenicity. The optical clarity of hydrogels permits the use of a vast assortment of photochemical methods to fabricate material structures or pattern biomolecules within the hydrogel matrix. Similarly, their high water content creates an environment conducive to the encapsulation of cells. Therefore, in this review, we discuss primarily the properties of hydrogel-forming polymers (**Table 1**) (**Figure 3**). When describing the properties of hydrogel materials, we first divide them into two main categories: natural and synthetic.

Natural polymers are often derived from native ECM components such as collagen (12, 17–19), fibrin (20–22), hyaluronic acid (HA) (23–26), or Matrigel™ (27–29), but they have also been created from nonmammalian sources such as algae (alginate) (9, 14) and seaweed (agarose) (30, 31). Natural hydrogel polymer materials have the advantages of high biocompatibility and degradability through natural enzymatic or chemical processes. In addition, materials derived from mammalian ECM contain natural ligands that allow for cellular adhesions; thus, they often do not require additional modifications to support cell growth and spreading. However, it can be difficult to decouple the effects of different biochemical cues and signaling molecules such as growth factors or adhesive sequences in these materials because they can exist naturally within the hydrogel matrix. This is especially true in matrices such as Matrigel™ for which the overall polymer makeup is only loosely known (32).

Alternatively, many synthetic polymers capable of forming hydrogels have also been developed to act as blank-slate materials, the biochemistry and mechanics of which can be custom-tailored via simple chemical modifications. Although poly(ethylene glycol) (PEG) is the most commonly explored synthetic polymer owing to its innate protein repulsiveness and the fact that it is already FDA approved for certain applications, several other hydrogel-forming polymers have been investigated. These include poly(2-hydroxy ethyl methacrylate) (PHEMA) (33, 34), poly(acrylamide)

Table 1 Properties of natural and synthetic hydrogel-forming polymers as related to tissue engineering

Polymer	Variants	Polymerization method(s)	Degradable	Supports cell adhesion?	Notes	Reference(s)
Synthetic polymers						
Poly(ethylene glycol) (PEG)	PEG-diacrylate (PEGDA)	Photo	No	No	Can be polymerized via Michael addition in the presence of a dithiol	37, 51, 104, 143, 149
	PEG-dimethacrylate (PEGDMA)	Photo	No	No	Can be polymerized via Michael addition in the presence of a dithiol	142
	PEG peptide	Generally photo	Yes, if protease-sensitive or photocleavable peptide is used	No		10, 15, 52, 58
Multiarm PEG (maPEG)	maPEG acrylate	Michael-type addition; photo	Enzymatic with MMP-sensitive peptide cross-linker	No	Requires dithiol cross-linker for Michael-type addition	37
	maPEG thiol	Michael-type addition	Enzymatic with MMP-sensitive peptide cross-linker	No	Requires diacrylate cross-linker	37
	maPEG azide	Strain-promoted azide-alkyne cycloaddition	Enzymatic with MMP-sensitive peptide cross-linker	No	Requires DIFO3 or similar cross-linker	68, 69, 37
	maPEG tetraDIFO3	Strain-promoted azide-alkyne cycloaddition	Enzymatic with MMP-sensitive peptide cross-linker	No	Requires diazide cross-linker; not commercially available	66, 67
Poly(acrylamide) (PAm)		Photo	No	No		35
Poly(*N*-isopropyl acrylamide) (PNIPAAm)		Photo	No	No	Thermally responsive	36
Poly(2-hydroxy ethyl methacrylate) (PHEMA)		Photo	No	No		33, 34

(*Continued*)

Table 1 (*Continued*)

Polymer	Variants	Polymerization method(s)	Degradable	Supports cell adhesion?	Notes	Reference(s)
Natural polymers						
Agarose		Thermal	No	No		30, 31, 156–59
Alginate		Ionic, Ca^{2+}	No	No	Oligomers of mannuronic acid (M) and guluronic acid (G) and other divalent cations can act as cross-linkers	9, 14, 79
Collagen		Thermal; pH	Enzymatic: MMPs and collagenase	Yes	Temperature and pH can be altered to adjust fiber size	12, 17–19
Fibrin		Enzymatic cleavage of fibrinogen by thrombin	Enzymatic: plasmin	Yes		20–22
Gelatin		Thermal; pH	Enzymatic: MMPs and collagenase	Yes	Hydrolyzed collagen	77, 78
	Gelatin methacrylate (GelMA)	Photo	Enzymatic: MMPs and collagenase	Yes		56, 134
Hyaluronic acid		Chemical; requires cross-linker	Enzymatic: hyaluronidase	No	A variety of cross-linkers can be used that can react with free hydroxyl or carboxylic acid groups	24
	Methacrylate/acrylate hyaluronic acid (MeHA/AHA)	Photo	Enzymatic: hyaluronidase; can incorporate MMP-sensitive cross-linkers	No	Methacrylates/acrylates linked via free hydroxyl groups	11, 23, 50
Matrigel		Thermal	Enzymatic: primarily MMPs and collagenase	Yes	Loosely known matrix with batch to batch variation	27–29, 32

Abbreviations: DIFO3, difluorinated cyclooctyne; MMP, matrix metalloproteinases.

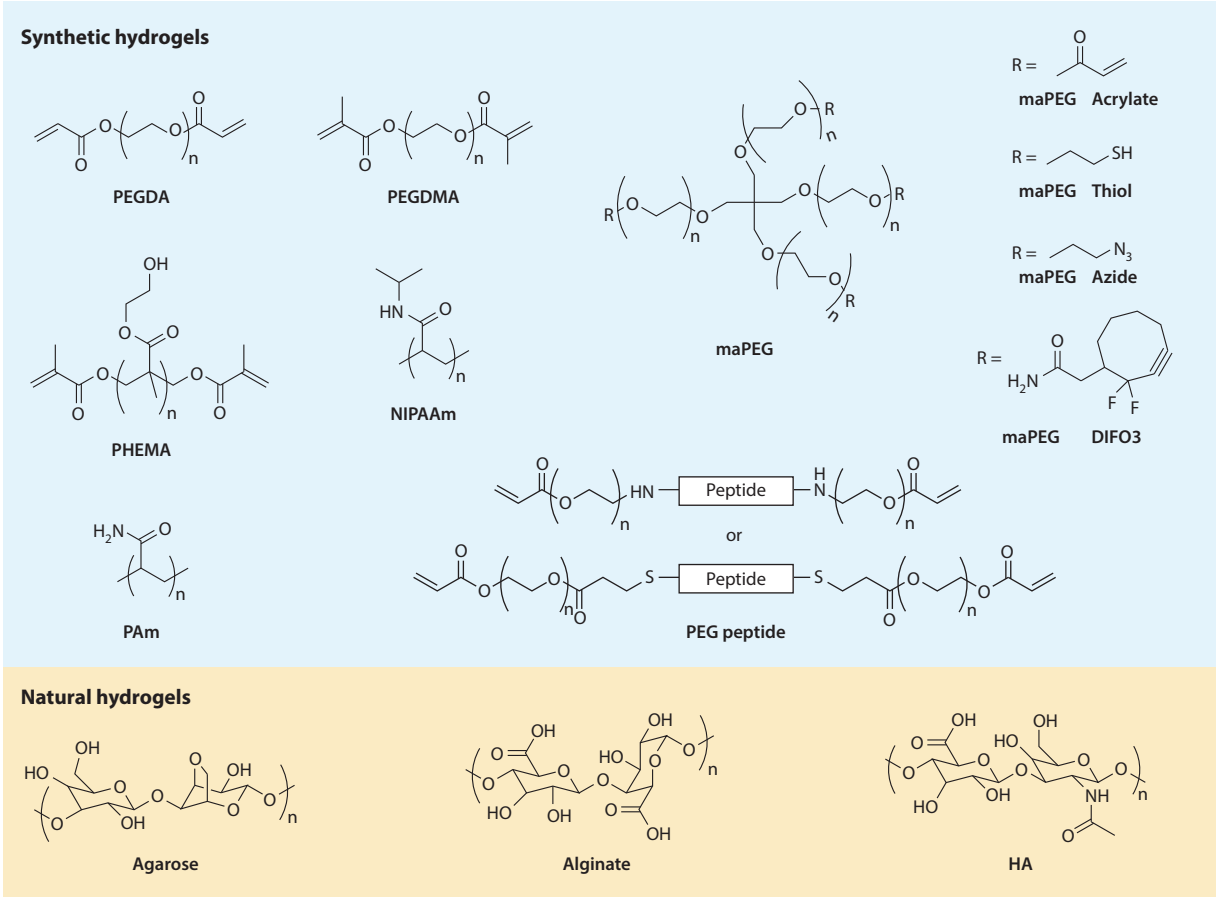

Figure 3

Chemical structures of common polymers for biofabrication. Abbreviations: DIFO3, difluorinated cyclooctyne; HA, hyaluronic acid; maPEG, multiarm PEG; NIPAAm, *N*-isopropyl acrylamide; PAm, poly(acrylamide); PEG, poly(ethylene glycol); PEGDA, PEG-diacrylate; PEGDMA, PEG-dimethacrylate; PHEMA, poly(2-hydroxy ethyl methacrylate).

(35), and poly(*N*-isopropyl acrylamide) (PNIPAAm) (36). These materials do not support cell adhesion, but they can be functionalized with ECM proteins (e.g., fibronectin or laminin) or ECM-mimetic peptides such as Arg-Gly-Asp-Ser (RGDS, or RGD) or Ile-Lys-Val-Ala-Val (IKVAV), which are derived from fibronectin or laminin, respectively (37). In addition to purely natural or purely synthetic materials, many natural/synthetic polymer hybrids have been created in the hopes of achieving "best of both worlds" material properties (38, 39). This hybridization has been further extended to incorporate non-polymer-forming proteins to create hydrogels that harness the mechanical and biochemical properties of the protein (40, 41).

2.1. Engineering Degradability in Biomaterials

For many tissue engineering applications, it is desirable to have the scaffold material degrade, allowing the material to be broken down as the scaffold material is replaced with cells or tissue and newly deposited ECM. Importantly, these degradation by-products must be biologically inert, so that they can be rapidly cleared after they have been broken down. In the case of polymer

degradability, there are two dominant mechanisms: (*a*) chemical, in which the polymer chain is broken down by chemical reactions such as hydrolysis, and (*b*) enzymatic, in which enzymes secreted by cells in culture recognize and cleave specific sites within biological polymers.

Although synthetic polymers have no inherent biological properties, some can undergo chemical degradation through bulk hydrolysis. Hydrolysis reactions are often catalyzed via acidic or basic conditions, but they can also often be tuned within physiologically relevant conditions (42). Poly(lactic acid) (PLA) blocks have been incorporated into PEG chains to imbue degradative properties through hydrolysis with predictable kinetics (43, 44). Similarly, ester (45, 46), thioether-ester (47), thiol-acrylate (42, 48), and thiol-allyl ether (49) linkages have been inserted within synthetic polymer macromers or used as cross-linking sites to take advantage of and tune hydrolytic degradation pathways.

Enzymatic degradative processes are normally seen with the use of natural materials where enzymes cleave either specific amino acid sequences, such as matrix metalloproteinases (MMPs) toward collagen, or biologically relevant chemical structures, such as hyaluronidase toward the disaccharide chains of HA. For materials that either are nondegradable, degrade under conditions not amenable to cell viability, or degrade via enzymes not secreted by the cultured cells, mimetic peptide sequences can be incorporated into the polymer structure to render the final hydrogels degradable. This technique has been used extensively to incorporate MMP- (11, 50–52) as well as plasmin-sensitive (53, 54) peptide sequences in both synthetic and natural polymer hydrogel networks. Furthermore, the peptide sequences can be modified to tune their MMP-specific degradation kinetics depending on the application (55).

2.2. Cross-Linking and Mechanics for Biomaterials

The mode of polymerization can have critical consequences for both the choice of a polymer system and the resulting hydrogel structure and mechanics. The mode is especially important because the mechanics of the materials should closely match the endogenous matrix of the cell or tissue niche being investigated. Most naturally derived polymers have their own inherent methods of gelation, such as thermal (agarose, collagen, Matrigel™, and gelatin), pH (collagen and gelatin), ionic (alginate), or enzyme-based (fibrin) cross-linking. For these materials, the mechanics of the resulting gel can be loosely controlled by adjusting the prepolymer density. However, the kinetics of these cross-linking processes can vary greatly, from several minutes to hours. Therefore, researchers have started functionalizing natural polymer materials with chemically cross-linkable side groups such as methacrylates (11, 56), thiols (57), or aldehydes (9). Synthetic polymers have been similarly modified to utilize multiple photo-cross-linking mechanisms such as acrylate-acrylate (58, 59), thiol-ene (45, 60, 61), or thiol-yne (62, 63). These polymerizations occur quite rapidly, often permitting the encapsulation of cells during the polymerization reaction. The reaction kinetics and matrix mechanics can be easily tuned based on the prepolymer concentration, cross-linking time, and/or photoinitiator concentration. In addition, several other chemical reaction–based chemical cross-linking methods, such as Michael-type addition (64, 65) and azide-alkyne cycloaddition-based click chemistry (66–69), have been effectively used to encapsulate cells with tunable kinetics and matrix mechanics.

3. CURRENT STRATEGIES FOR 3D BIOFABRICATION

In light of the need for improved biomaterials-based cell culture strategies, many biofabrication techniques aim to better capture the complex heterogeneous nature of endogenous cells,

tissues, and organs for tissue engineering and regenerative medicine applications. By using the biomaterials mentioned above, these biofabrication strategies are used to develop scaffolds with well-defined 3D topologies and geometries to incorporate biomolecules within the 3D matrix with specific orientation and concentration. A scaffold with high porosity and tunable pore sizes and mechanical strength is desirable for tissue engineering applications. Large pores allow easy diffusion of molecules, waste products, and gases within a 3D scaffold. They also help with cell migration, spreading, and proliferation (70). **Table 2** summarizes the different biofabrication techniques that we discuss in this review.

3.1. Traditional Biofabrication Techniques

A multitude of fabrication technologies are available to create 3D scaffolds by using both synthetic and naturally occurring biomaterials. An overview of some of these traditional or conventional techniques is provided below. These techniques aim to create scaffolds that mimic the physiological microenvironments experienced by the cell. In all the traditional technologies, fabrication of the scaffold occurs first, followed by seeding of the cells in the scaffold.

3.1.1. Solvent casting or particle leaching. Solvent casting is a technology in which a polymer solution is dissolved in a solvent with uniformly distributed salt particles of a specific size (71). At first, the solvent is allowed to evaporate, leaving behind a composite with uniformly distributed salt particles. This polymer matrix is then immersed in water to allow leaching of the salt particles. This results in the formation of a highly porous uniform 3D matrix that can be used to seed different types of cells. The pore size of the scaffold is strictly a function of the salt particles' diameter and is often optimized for the specific application. The resulting polymer matrix is 99.9% salt-free, and it can have over 90% porosity and median pore diameters of up to 500 μm (71, 72). Park et al. (73) fabricated a block polymeric scaffold of PEG and poly(E-caprolactone) (PCL) using sodium chloride as the porogen and dimethyl sulfoxide as the solvent. Keeping the total polymer concentration constant, the authors varied the ratios of PEG:PCL to obtain hydrogels with different mechanical properties. By seeding chondrocytes in these scaffolds, they showed optimal cartilage formation for the scaffold with the highest hydrophilicity, thus supporting the importance of scaffold properties in determining cellular functionality. Mehrabanian and colleagues (72) fabricated nanohydroxyapatite (nHA) nylon 6,6 composite scaffolds using particle leaching. The microstructure of the scaffold showed a very high porosity with pore size ranging from 200 to 500 μm, which was similar to the size of the porogen used. The mechanical properties of the scaffold were similar to those of cortical bone, and thus the authors claimed that the scaffold would be ideal for studies involving bone development. Another study, done by Ford et al. (74), used a salt-leached poly(lactic-co-glycolic acid) (PLGA) scaffold as a template around which the authors synthesized a hydrogel by cross-linking PEG with poly-L-lysine. This hydrogel was then degraded by sodium hydroxide to create a highly porous hydrogel scaffold that was used for seeding the cells. Endothelial cells were seeded in this hydrogel network in vitro, and the authors reported efficient microvessel formation.

One of the biggest advantages of this technique is that the pore size and in turn, the mechanical properties of the scaffold can be easily tuned by controlling the size and geometry of the porogen (70). However, the main disadvantage of the technique is the use of cytotoxic organic solvents for fabrication of these scaffolds. The scaffold needs to be repeatedly washed to ensure complete removal of the solvents and minimize cell death.

Table 2 Overview of the different biofabrication techniques discussed in this review

Fabrication scheme	Principle of operation	Cell encapsulation during fabrication	Advantage(s)	Disadvantage(s)	Key references
Traditional techniques					
Solvent casting or particle leaching	Allow leaching of porogen from a polymer matrix to form 3D macroporous scaffolds	No	Pore size of the scaffold can be controlled by adjusting the parameters of the porogen	Use of cytotoxic solvents for scaffold fabrication	72, 74, 75
Freeze drying	Creation of thermodynamic instability in a 3D scaffold causing phase separation and pore formation	No	Pore size can be easily controlled by tuning the freezing regime	Use of cytotoxic solvents and lengthy timescales for scaffold fabrication	76, 79, 80, 84
Gas foaming	Nucleation and growth of bubbles in a 3D polymer matrix to create macroporous scaffolds	No	Use of relatively inert foaming agents without employing cytotoxic chemicals; pore size can be controlled by adjusting the operating gas pressure	Minimal pore interconnectivity at times, which can pose diffusion limitations for the encapsulated cells	85, 88, 90, 92
Bioprinting					
Drop based	Layer-by-layer drop-based deposition of polymers (with or without cells) onto a substrate controlled by an automated stage	Yes	Fast deposition of layers over relatively large areas; automated to construct complex architectures	Spreading and deposition of droplets generally faster than gelation kinetics; possible heating during drop formation, limiting its polymer and cell compatibility	92–97
Extrusion	Layer-by-layer printing by direct contact of the print head with the substrate, controlled by translation of an automated stage	Yes	Gentler handling of polymers and cells; automated to allow printing large complex structures	Slower printing method; only compatible with a few polymer systems	34, 35, 98–100
Photolithography					
Mask based	Use of a mask to photopolymerize and cross-link polymers, resulting in a 3D scaffold	Yes	Uniform cell encapsulation; good spatial and temporal control of reaction kinetics; easy control of pore size by varying the polymer type and concentration	Requires manual and prefabrication of multiple photomasks for multilayered scaffold constructs	11, 31, 105, 109, 137, 138

(*Continued*)

Table 2 (*Continued*)

Fabrication scheme	Principle of operation	Cell encapsulation during fabrication	Advantage(s)	Disadvantage(s)	Key references
Photolithography					
Stereolithography	Maskless photopolymerization to cross-link polymers, generating a 3D scaffold	Yes	Automated and fast processing; easy fabrication of structures with different parameters (pore size, elastic modulus) by changing the polymer parameters	Feature size that can be polymerized limited to the beam width of the laser	107, 108, 142–146
Multiphoton	Scanning a femtosecond pulsed laser within 3D hydrogels to localize photochemistries for immobilization or photodegradation	Yes	Control local biochemistry or cleave photolabile groups for degradation with high lateral and axial resolution; can be automated to create complex patterns	Lateral resolution higher than axial (~1 μm versus 5–6 μm); limited depth of patterning (~1 mm)	15, 30, 66–69, 102, 105, 155–161, 163

Abbreviation: 3D, three dimensional.

3.1.2. Freeze-drying. Freeze-drying, also known as lyophilization, is a process in which a polymer (synthetic or natural) solution is cooled down below its freezing point, leading to the solidification of the solvent molecules (75, 76). This forces the polymer to aggregate in the interstitial spaces of the scaffold. The solvent is then evaporated via sublimation, and this leaves behind a highly porous polymeric structure with interconnected pores that can be used for seeding the cells. The pore size of the scaffold is a function of the freezing regime, the concentration of the polymer, the size of the ice (solvent) crystals, and the pH of the solution (77–79). In order to reduce the solubility and the degradation rate of naturally occurring polymers (collagen, alginate, gelatin), they are generally cross-linked by UV radiation (80) or by chemicals such as gluteraldehyde (78), citric acid (81), and carbodiimide (82) prior to cell seeding. Shapiro & Cohen (79) fabricated 3D alginate porous sponges by lyophilization for studying cellular interactions. They showed that the alginate sponges had pores ranging from 70 to 300 μm and were ideal for the culture of fibroblasts. Lai and coworkers (82) developed cross-linked porous gelatin hydrogels by freeze-drying. They reported that rabbit corneal endothelial cells showed unfavorable tissue material interactions for the hydrogel discs with higher gelatin concentration, whereas favorable interactions were seen for hydrogels with lower gelatin concentrations. By increasing the gelatin concentration, the authors reduced the pore size of the hydrogel, which, in turn, led to hostile tissue material interactions.

Even though a variety of polymers can be freeze-dried and used as a scaffold to investigate cell–matrix interactions, the lengthy timescales and high energy consumption of this process (83) limits its use for tissue engineering applications. In addition, this technique also uses cytotoxic solvents for mixing the polymer, and any exposure to residual solvents can potentially be lethal for the cells.

3.1.3. Gas foaming. Gas foaming is a biofabrication technique in which a polymeric scaffold is saturated with a foaming agent such as carbon dioxide (84), nitrogen (85), or water (86) at high pressures. The pressure of the foaming agent is decreased, which leads to a decrease in the solubility of the gas in the polymer. Gas bubbles are formed and grow in the polymer as a result of this thermodynamic instability (87). A porous structure with pores sizes ranging from 100 to 500 μm can be formed in the scaffold using this technique (88). Harris and colleagues (89) fabricated disks of PLGA using gas foaming. Smooth muscle cells readily attached to these polymeric scaffolds and formed 3D tissues within the porous structure of the scaffold. Kim et al. (90) fabricated a porous biphasic calcium phosphate (BCP) scaffold using gas-foamed polyurethane as a template. Both in vivo and in vitro tests confirmed that the BCP scaffold was biocompatible and could be used for bone differentiation and regeneration. Nam and coworkers (91) fabricated highly porous PLA biodegradable scaffolds using gas foaming and reported that cultured rat hepatocytes exhibited about 95% seeding efficiency and up to 40% viability on day 1 after the seeding.

One of the biggest advantages of this technique for tissue engineering applications is the use of relatively inert foaming agents without the involvement of cytotoxic solvents. However, it has been reported that only 10–30% of the pores are interconnected in the scaffold, which may pose diffusion limitations for encapsulated cells in the scaffold (87).

3.2. Bioprinting

Bioprinting has quickly become an attractive method to rapidly fabricate complex architectures in a top-down approach over large length scales. Here, prepolymer solutions, cells in prepolymer suspension, or cell aggregates/spheroids—the "bioink"—are deposited onto a substrate, sometimes referred to as "biopaper," in a layer-by-layer process to build 3D constructs analogous to tissues or organs (57, 92, 93). There are two basic methods of bioprinting: drop based and extrusion. In drop-based bioprinting, sometimes referred to as inkjet printing owing to its origins in modified inkjet printers (94), a mechanical print head deposits the bioink in droplets that can then coalesce and gel to form polymeric structures (**Figure 4*a***). Extrusion bioprinting utilizes a mechanical extruder to continuously deposit the bioink as the extruder or stage is moved (**Figure 4*b***), permitting the use of high cell densities with gentler processing but at reduced speeds as compared with drop-based techniques (57). Next we describe several polymer systems that have been effectively used within these two bioprinting strategies to biofabricate complex 3D polymer culture systems.

3.2.1. Drop-based bioprinting. Drop-based bioprinting has become increasingly popular owing to the speed at which it can construct scaffolds and biomaterials with elaborate 3D architectures. In fact, this speed makes the technique difficult to apply to many polymer systems, as it requires the gelation time to be faster than, or at least similar to, the drop deposition time. One of the first demonstrations of this technology showed that cell viability was maintained when suspensions of Chinese hamster ovary (CHO) cells and primary embryonic rat motoneurons in phosphate buffered saline (PBS) were deposited onto a biopaper substrate of collagen or agar using a modified ink jet printer (95). This process was later expanded to print endothelial cells and fibrin scaffolds simultaneously to generate microvascular structures (96). Using a 3D printer–based system, an alginate bioink printing method deposits alginate prepolymer onto a gelatin substrate that acts as a Ca^{2+} reservoir. The alginate prepolymer is then introduced dropwise to the surface and forms a gel as the Ca^{2+} ions diffuse into the droplet. To minimize droplet spreading effects on structures, an alternative drop deposition algorithm allows printing of vessel-like structures (14). Villar et al. (97) recently demonstrated the ability to print complex 3D geometries by generating picoliter aqueous

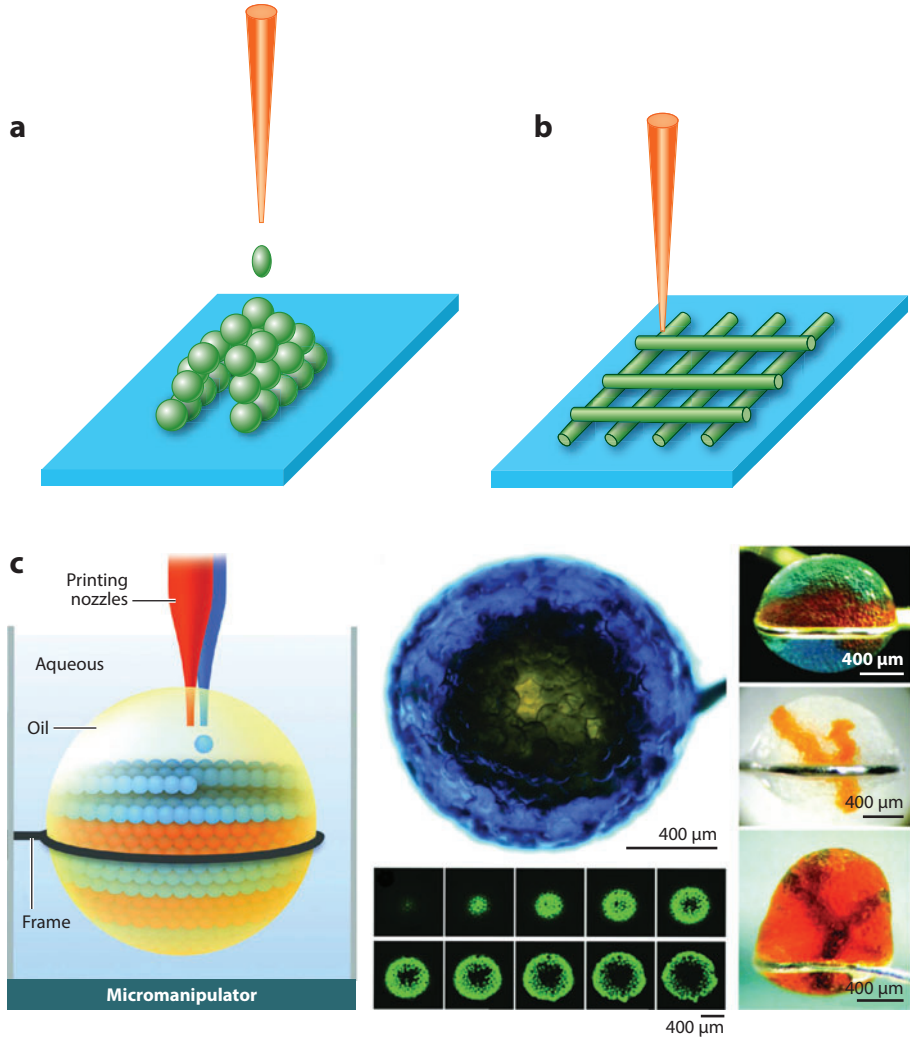

Figure 4

Bioprinting strategies for biofabrication. (*a*) Schematic of droplet-based bioprinting, in which 3D structures can be rapidly constructed through the controlled deposition of polymer droplets. (*b*) Depiction of extrusion bioprinting, in which the polymer is deposited from direct contact of the print head with the substrate. (*c*) An example of droplet-based bioprinting in which aqueous droplets were released within an oil environment to build spherical structures with multiple colored droplets and to create several different 3D architectures (97). (Reprinted with permission from the American Association for the Advancement of Science.)

droplets in lipid-containing oil, creating arrangements of lipid bilayer–coated spheres. These lipid bilayers were then modified to contain membrane proteins as well as to form interconnected networks. Furthermore, osmotic gradients were introduced to fold the droplet-based structures into several unique 3D arrangements (**Figure 4*c***) (97). Although drop-based printing offers a rapid method for fabricating large structures, it requires fast polymerization kinetics, which limits the polymers that can be used.

3.2.2. Extrusion bioprinting. In extrusion bioprinting, or direct ink write (DIW), a stage, or surface, is moved in a directed fashion (generally by computer), controlling the spatial deposition of the bioink from a nozzle to create materials of predetermined architecture (98). Biofabrication with DIW techniques is an efficient method for the creation of colloidal assemblies (99) or functional oxide assemblies (100), and it utilizes a prepolymer ink solution containing the monomers (or oligomers), cross-linker molecules, and initiators. During this process, the nozzle is followed by a UV illumination source to photopolymerize the ink into its final structure. The Lewis group has used this technology to write (*a*) 3D acrylamide hydrogel structures to support the culture of 3T3 fibroblasts (35) and (*b*) PHEMA hydrogel structures to direct and align primary hippocampal neurons (34). Although these studies demonstrate the modularity and applicability of DIW techniques toward biofabrication, the resulting materials require a final poly-L-lysine coating to promote cell adhesion. Extrusion bioprinting has similarly been used to construct complex 3D architectures for tissue engineering. For example, Norotte et al. (93) used extrusion bioprinting with agar-rod cellular spheroids to create artificial vascular tubular grafts that exhibited heterogeneous cell distributions. Though not as fast as drop-based printing, extrusion methods are gentler on cells and compatible with more polymers. However, the extrusion process can limit the final architecture and geometry of the polymer.

3.3. Photolithography Techniques

Photolithography techniques use light or photons to transfer the geometric shapes of a mask to a light sensitive surface. The origins of this technique can be traced back to the modern semiconductor industry, where photolithography has been extensively used to create intricate patterns on thin oxide films or bulk substrates. For biomedical applications, photolithography can be used either to create a 2D scaffold for the growth of cells (101) or to encapsulate the cells in a 3D network of polymers (102). Some of the advantages of photolithography systems are their ability to uniformly encapsulate cells throughout the scaffold, their minimal heat production, and their good spatial and temporal control of the reaction kinetics (103). As a result, photolithography has been widely used in tissue engineering to create 3D scaffolds for culturing multiple cell types, such as hepatocytes (104), fibroblasts, C2C12 myoblasts, endothelial cells, cardiac stem cells (56), HT1080 fibrosarcoma cells (105), mouse embryonic stem cells (mESCs) (106), and hippocampal neurons (107). Despite photolithography's wide use in tissue engineering, it does have some drawbacks. In any photolithography system, the incident light is absorbed by a photoinitiator, which creates a reactive species (free radical) that initiates the chain reaction. Depending on the dose, these free radicals can be cytotoxic to the cells, especially when the polymerization is done in the presence of cells (103, 108). In addition, after light illumination, there will be a gradient of photoinitiator for thick samples, which can lead to spatial nonuniformities in the mechanical properties of the scaffold (109, 110). Nevertheless, photolithography techniques have been successfully employed for creating 3D scaffolds for tissue engineering, and we discuss some of them in the sections below.

3.3.1. Mask-based photolithography. Mask-based photolithography, as the name suggests, uses a patterned mask to illuminate selected regions of a polymer. The mask is fabricated using standard lithography techniques that were developed for the microelectronics industry. Mask-based photolithography involves exposure of the prepolymer solution to UV light. Only regions of the solution that are exposed to light polymerize and cure to form a network of 3D porous scaffolds. This assembly is then immersed in a buffer to wash off any unnecessary unpolymerized solution (111). A variety of both natural (modified) and synthetic polymers can be photopolymerized using this method (112–115).

It is well documented that mammalian cells are sensitive to their microenvironmental cues, such as stiffness (116, 117), geometry (118, 119), topography (120–123), roughness (124–127), and ligand density (128, 129) in 2D. Mask-based photolithography allows tuning of these matrix parameters for both 2D and 3D hydrogels (130, 131). Khetan et al. (11) generated regions of soft and stiff 3D HA hydrogels in the same construct using multiple modes of peptide and UV cross-linking. Human MSCs (hMSCs) encapsulated in these hydrogels showed stiffness dependence differentiation into osteogenic or adipogenic lineages in the HA hydrogels. Interestingly, hMSCs in the stiffer regions of the hydrogel differentiated into adipocytes, whereas the ones in the softer regions differentiated into osteocytes. These results contrast with previously published reports (9, 132). In addition, cell spreading was observed only in the permissive-UV (soft) regions of the hydrogel. Nevertheless, this study showed that stiffness gradients in 3D hydrogels can be used to control the fate of mammalian cells. Another way to modulate the mechanical properties of a 3D hydrogel is by tuning the degree of cross-linking and the prepolymer concentration. Nichol and coworkers (133) fabricated methacrylated gelatin (GelMA) hydrogels of physiologically relevant stiffness (117, 134) by changing the degree of methacrylation (from 20 to 80%) and GelMA concentration (from 5 to 15%). 3T3 fibroblasts encapsulated in these micropatterned 3D scaffolds showed viability in excess of 90% for the softest hydrogel (5% GelMA), whereas a viability of only 75% was recorded for the stiffest hydrogels (15% GelMA).

In another study, Liu Tsang et al. (104) photopolymerized PEG hydrogels with cell-adhesive RGD ligands using a multilayer photopatterning platform. Hepatocytes seeded in the photopatterned hydrogels showed improved viability over bulk (nonpatterned) hydrogels because of improved nutrient transport in the patterned hydrogels. In addition, urea and albumin production was also higher for pattered hydrogels versus nonpatterned hydrogels. This report showed that by spatially patterning cells in 3D hydrogels, their viability and functionality can be improved. There have been a number of other studies that have encapsulated cells in patterned 3D hydrogel scaffolds and studied cell migration (31), cell proliferation/spreading (135), and cell elongation/fibril formation (136).

Mask-based photolithography also allows for controlled coculture of multiple cell types in 3D hydrogels. Hammoudi and colleagues (137) used this technique to fabricate oligo(PEG-fumarate):PEG-diacrylate (PEGDA) hydrogels with high spatial resolution. Primary tendon/ligament fibroblasts and marrow stromal cells were encapsulated in these hydrogels and showed a high degree of viability over a period of 14 days. Although paracrine interactions between the two cell types were not investigated, this fabrication modality can be used to study both homotypic and heterotypic cell–cell interactions, which could be useful for a plethora of biomedical applications.

One of the major disadvantages of a mask-based photolithography system is the lack of automation. Photomasks need to be manually changed and aligned after every layer for multilayered scaffolds. In addition, multiple photomasks need to be prefabricated, which can be very expensive and time-consuming.

3.3.2. Stereolithography. Stereolithography (SL) is a maskless photopatterning technique introduced in the 1980s to create prototypes for the manufacturing industries (138). It is a computer-aided design (CAD) technique used frequently by the rapid prototyping industry and at least in the past decade or so, for biomedical applications (138, 139). The basic working principle of this technology is as follows (140): The design of the structure/scaffold to be fabricated is first developed by a 3D computer drawing software. For very intricate 3D designs, magnetic resonance imaging (MRI) or computed tomography (CT) can also be used. This design is then processed by software and sliced into a number of layers that are 25–100 μm thick. The data are then passed to the SL apparatus (SLA), where each layer is built one at a time by the ultraviolet (UV) laser.

The SLA stage/elevator then moves up, and the second layer is cured in the same way. This process continues until the entire structure is complete. SL offers some unique advantages over mask-based photolithography systems (106). As a maskless technology, SL does not require fabrication of a physical mask, thus reducing both the cost and time required for scaffold fabrication. Also, with this automated technique, there is precise control over the thickness of the scaffold. SL allows the rapid fabrication of structures ranging in size from a few hundred micrometers to a few millimeters.

One of the first studies that demonstrated the use of SL for biomedical applications was performed by Dhariwala and coworkers (141). They encapsulated CHO-B2 in a poly(ethylene oxide) and PEG-dimethacrylate (PEGDMA) hydrogels of simple geometries and reported high cell viabilities. Even though the study demonstrated only viability of cells, it was the first of its type and showed that SL could be used for tissue engineering applications. Arcaute et al. (142) expanded on this study by encapsulating human dermal fibroblasts in photo-cross-linked PEGDMA hydrogels of complex geometries, which could be used as nerve guide conduits. The authors found viability close to 90% after 24 h (**Figure 5*a***). The Bashir group modified the commercially available SLA to show the long-term viability of 3T3 cells in PEGDA hydrogels of different molecular weights (143). They found that cellular viability was a close function of the hydrogel pore size: Higher pore sizes (higher molecular weights) resulted in better cell viability. In addition, by adding cell-adhesive peptide sequences of RGDS to the polymer backbone, the authors demonstrated increased cell viability, proliferation, and spreading. Seck et al. (144) fabricated biodegradable hydrogels by polymerizing PEG/poly(D,L-lactide) macromers with SL. MicroCT revealed that the average pore size of the hydrogel was 423 μm, with more than 90% of the pore volume accessible from the outside of the scaffold. hMSCs were able to attach and spread on these scaffolds, confirming that these biodegradable scaffolds fabricated by the SLA could be used for tissue engineering applications.

Kong and colleagues (145) encapsulated 3T3 fibroblasts in microvascular stamps fabricated by the SLA to control the growth of neovessels. A desired geometrical pattern of neovessels was achieved on the chick embryo chorioallantoic membrane based on the 3D geometry of the stamp. The 3T3 fibroblasts encapsulated in the microvascular stamps released proangiogenic growth factors that were localized to the geometry of the stamp. The release of growth factors led to sprouting of new blood vessels on the embryo's membrane, and this growth of the neovessels was a function of the hydrogel's microchannel diameter (**Figure 5*b***). The authors believe that this work could be used for the development of the next generation of bandages—ones that would form new blood vessels for enhanced recovery of the wound. Zorlutuna et al. (107) used SL to fabricate biodegradable hydrogels and encapsulated primary hippocampal neurons (HNs) with skeletal muscle myoblast cells (MCs) to study heterotypic cell interactions. The hydrogels that had both HNs and MCs in the same scaffold showed much higher choline acetyltransferase (ChAT) activity than the hydrogels that were cultured in conditioned media (**Figure 5*c***). SL enabled multicell encapsulation and showed that spatiotemporal interactions are important in cellular systems. In addition, this methodology can be used to investigate cellular interactions in 3D microenvironments.

Although SL has emerged as a powerful biofabrication technology in the past few years, the minimum feature size that can be fabricated by the conventional SLA is limited to the beam width of the laser. Most commercially available lasers have a beam width of about 250 μm (146). As a result, 3D microscale tissue organization cannot be achieved using the commercially available SLA. To circumvent this problem, Bajaj et al. (106) combined SL with dielectrophoresis (DEP) to pattern cells with a high degree of 3D spatial control. The cells were first patterned by the DEP forces and then polymerized by the SLA to mimic the elements of native tissue (**Figure 5*d***). In

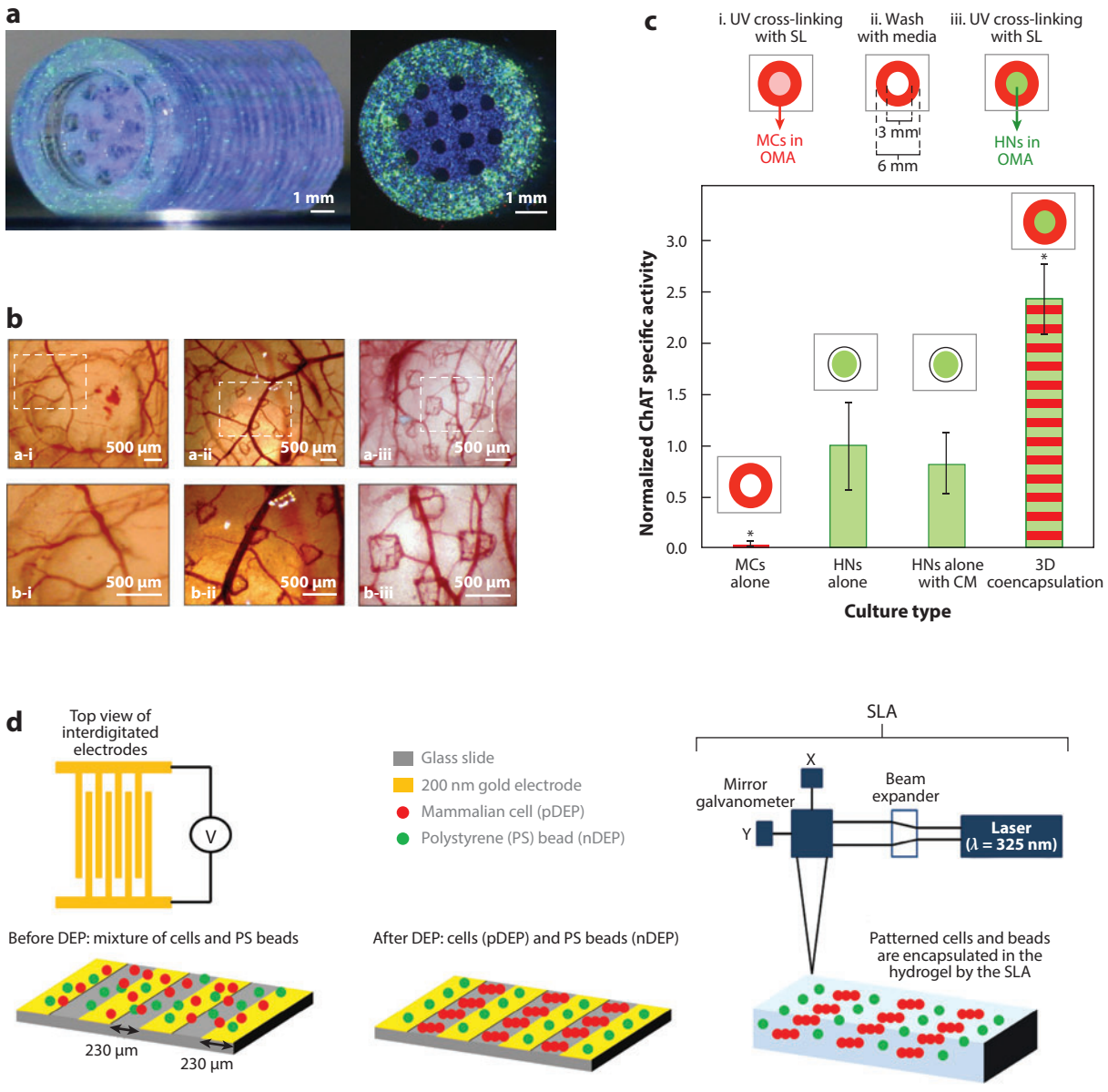

Figure 5

Maskless stereolithography for biofabrication. (*a*) Multilumen PEG hydrogel conduit with fluorescent particles having an outer diameter of 5 mm and an inner diameter of 3 mm (*left*, isometric view; *right*, top view) (142). (*b*) Bright-field images of neovessels formed under hydrogels containing microchannels of the following diameters: 0 µm (a-i), 300 µm (a-ii), and 500 µm (a-iii). The implant sites from the top row are magnified in the bottom row (b-i, b-ii, and b-iii) (145). (*c*, *top*) Schematic outline of the SL fabrication process. (*bottom*) ChAT specific activity of HNs in different culture conditions (107). (*d*) Schematic showing the overall process of fabricating 3D spatially patterned hydrogel constructs by combining SL with DEP (106). Abbreviations: 3D, three dimensional; ChAT, choline acetyltransferase; CM, conditioned media; DEP, dielectrophoresis; HNs, hippocampal neurons; MCs, myoblast cells; OMA, oxidized methacrylic alginate; PEG, poly(ethylene glycol); SL, stereolithography; SLA, stereolithography apparatus; UV, ultraviolet. (Reprinted with permission from Springer and John Wiley and Sons.)

addition to single cells, this technique also allowed patterning of cell spheroids in 3D hydrogels, making it a very robust platform for tissue engineering applications. Also, new SL systems with improved resolution are now commercially available. These high-resolution SLAs have an accuracy of about 20 μm (138). In addition, recent years have also seen the use of the microSLA for tissue engineering applications (147–149). With the microSLA, submicrometer-sized features can be fabricated in hydrogels, thereby allowing microscale tissue organization (150).

In addition to tissue engineering and regenerative medicine, SL can also be used for the development of soft robotics and biological machines. Recently, the Bashir group used the SLA to fabricate PEGDA hydrogel–based biological robots, or bio-bots, that were capable of spontaneous locomotion when seeded with rat cardiomyocytes (151). These bio-bots were also capable of attaining speeds of up to 236 μm/s with an average displacement of 354 μm per power stroke. The authors also claimed that in the future, these muscle-based bio-bots can be combined with sensory neurons to create in vitro neuromuscular junctions that could be used to sense and neutralize toxins. The SLA has the potential to fabricate different types of cellular machines that could have applications in a broad spectrum of disciplines, such as biosensing, drug discovery, energy harvesting, and environmental remediation.

3.3.3. Multiphoton lithography. Maskless lithography using a focused laser (31, 152) or confocal microscope (105) has been shown to offer high lateral (*x-y*) resolution but little to no control over the axial (*z*) direction. To overcome this limitation, many photochemistries have been expanded to multiphoton-based approaches, which are capable of confining the photochemical reactions in 3D. Whereas in single-photon absorption systems, a fluorophore is excited by one photon of a specific energy level, in multiphoton (or two-photon) processes, multiple photons of lower energy are needed to excite the fluorophore; this is known as the multiphoton (or two-photon) effect (**Figure 6*a*,*b***). For multiphoton lithography, the fluorophore is replaced by a photoinitiator to generate a free radical, which can be used in many of the photopolymerization methods described in Section 2.2. Because the absorbance of multiple photons must occur nearly simultaneously, this two-photon effect has a probability of occurrence that scales with the square of the laser intensity. With traditional, low-intensity, continuous-wave lasers, this is a very rare event even at the laser's focal point. Therefore, specialized femtosecond pulsed lasers are needed to generate intensities at their focus orders of magnitude higher than those of their continuous-wave counterparts while maintaining similar average power (153, 154). Common photochemical reactions used in multiphoton lithographic techniques are illustrated in **Figure 6*c***.

The first demonstration of multiphoton patterning within hydrogel structures was performed by Hahn et al. (105), who were able to control the mechanics and the biochemistry of PEGDA hydrogels by patterning either low-molecular-weight PEGDA monomers or acrylate-PEG-RGDS, respectively, using the multiphoton effect to initiate localized acrylate polymerizations. An example of this can be seen in **Figure 6*d***. Use of MMP-sensitive PEG hydrogels allowed the RGDS patterns to guide the invasion of surface-seeded HT-1080 fibrosarcoma cells into the hydrogel. Acrylate-PEG-RGDS patterns were similarly capable of guiding the 3D migration of human dermal fibroblast migration in MMP-sensitive PEG hydrogels from an encapsulated fibrin clot (102). Two-photon patterning of acrylate functionalized biomolecules was later shown to be amenable to serial patterning of multiple biomolecules in the presence of encapsulated cells with 1–2-μm and 5.4-μm precision in the lateral and axial directions, respectively (15, 155).

To separate the polymerization and patterning chemistries, the Shoichet group developed coumarin-derivatized agarose, in which a coumarin analogue can act as photolabile protecting groups for sulfahydryl (156) and amine groups (157). Using multiphoton irradiation, Wylie &

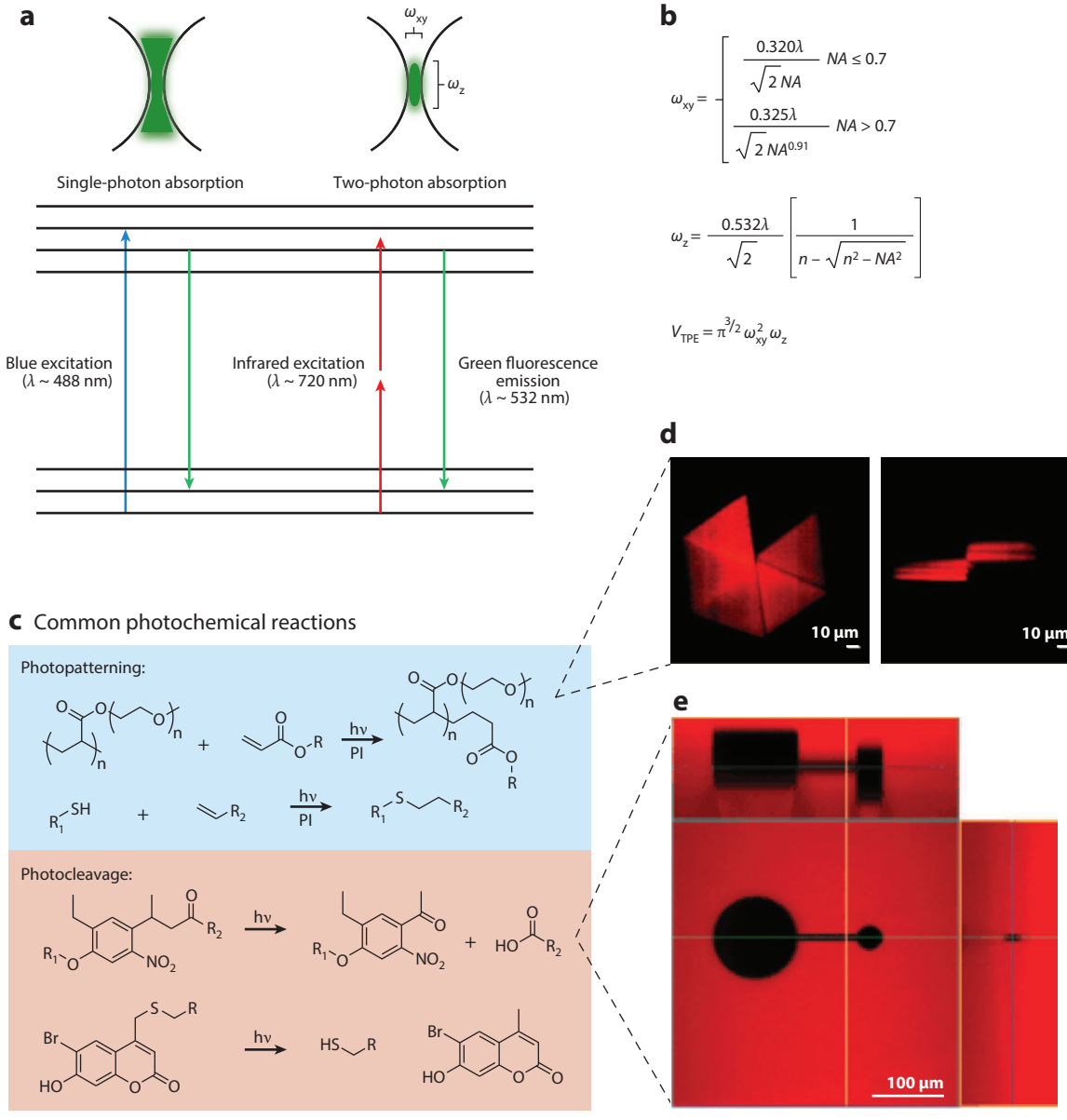

Figure 6

Multiphoton-based patterning and degradation of hydrogel environments. (*a*) Illustration of the two photon effect—that is, the absorbance of two photons using half the energy required by a single-photon absorption event—which yields a small excitation volume (V_{TPE}) described by the lateral (ω_{xy}) and axial (ω_z) dimensions. (*b*) The basic equations that govern the multiphoton excitation volume (V_{TPE}) and its parameters (ω_{xy} and ω_z), where *NA* is the numerical aperture of the microscope objective, λ is the wavelength of the excitation light, and *n* is the refractive index of the material. (*c*) The chemical reaction mechanisms commonly employed for two-photon patterning and degradation/cleavage techniques. PI indicates that a photoinitiator molecule is required for the reaction to proceed. (*d*) 3D projection of two-photon patterning using acrylate-based polymerization mechanisms to incorporate fluorescently labeled acrylate-PEG-RGDS molecules within PEG hydrogels. (*e*) An example of two-photon photodegradation in PEG hydrogels through the incorporation and photocleavage of a nitrobenzyl ether–based compound (160). Abbreviations: 3D, three-dimensional; PEG, poly(ethylene glycol); PI, photoinitiator. (Reprinted with permission from the American Association for the Advancement of Science.)

Shoichet (158) cleaved these coumarin-based protecting groups within agarose hydrogels, leaving free sulfahydryl moieties to react with maleimide groups or form disulfide bonds. This technique was used to pattern VEGF gradients to guide endothelial cell migration and tubule formation (30). Later, this technique was expanded to allow the patterning of multiple biomolecules utilizing maleimide-functionalized streptavidin and barnase proteins. In the latter process, the two proteins were patterned serially, allowing the agarose hydrogel to be incubated with biotin- and barstar-fused growth factors, which can then bind to streptavidin and barnase, respectively, to promote retinal precursor cell invasion (159). However, owing to the gelation mechanism of agarose, patterning was performed in the absence of cells.

The Anseth group has developed copper-free click-based hydrogels, which utilize strain-promoted alkyl-azide cycloaddition (SPAAC) to polymerize PEG hydrogels, that also offer the advantage of orthogonal polymerization and patterning chemistries. Using orthogonal click-based thiol-ene photocoupling, the group was able to pattern cysteine-terminated biomolecules to allyloxycarbonyl groups in protease-sensitive hydrogels (68). Furthermore, by incorporating a photolabile nitrobenzyl ether–derived group into the hydrogel backbone, the authors were able to selectively degrade the hydrogels using laser scanning two-photon microscopy (**Figure 6*e***) (160) and perform this in parallel with the thiol-ene patterning chemistry in the presence of hMSCs (66). Although multiple studies have successfully patterned multiple biomolecules in a serial fashion (15, 155, 159), Deforest et al.'s (66, 67) work was the first to demonstrate multiple photochemistries (thiol-ene photocoupling and nitrobenzyl ether photodegradation) in parallel. The authors have similarly incorporated this photolabile group on the N terminus of an RGD peptide to create a method to reversibly pattern biomolecules of interest (67).

Although these multiphoton patterning strategies offer a straightforward method to encode localized properties within hydrogel networks, they are difficult to scale to large materials (i.e., larger than a few millimeters). Also, the serial addition or patterning of multiple biomolecules can be time-consuming, limiting the overall complexity of the material environment. Therefore, it would be of interest to create new or adapt existing wavelength-specific photochemistries for parallel multiphoton patterning. This capability would enable greater spatial control as well as temporal modification of the hydrogel microenvironment.

Utilizing methods similar to these two photon-based patterning technologies, the Shear group has developed a direct write technology that uses a femtosecond pulsed laser source in conjunction with a photosensitizer (as opposed to photoinitiator), which chemically cross-links protein solutions into polymeric structures (161). As opposed to using classical photo-cross-linking groups, this method takes advantage of several possible amino acid side chains to create the final polymer structure (161–163). This technique is excellent at creating high-resolution (~1-μm) self-supporting structures, but it has also been utilized as a patterning technique within HA hydrogels to immobilize biotinylated bovine serum albumin (BSA) that can be detected with neutravidin and further functionalized with biotinylated peptides (163). Owing to the promiscuity of the cross-linking chemistry involved, this method is difficult to multiplex. Nonetheless, it offers an intriguing method to pattern diverse functionalities within 3D hydrogels.

4. PERSPECTIVES AND CHALLENGES

All the biofabrication techniques discussed above aim to create scaffolds that closely mimic the physiological microenvironments experienced by cells. However, the next generation of scaffolds must monitor the cells within these 3D microenvironments in real time. Unlike current scaffolds, which are passive in nature, the next generation of scaffolds must be active, monitoring the bioactivity of the embedded cells and even responding accordingly. A number of studies have used

electronic sensors to monitor the physiology of cells on 2D planar surfaces (164–167); however, integrating these electrical sensing moieties in 3D macroporous scaffolds has been a real challenge. Only recently, a report from Tian et al. (168) made the first step toward creation of a bioactive 3D macroporous scaffold. They successfully integrated silicon-nanowire field-effect transistors (FETs) with both natural (collagen, alginate) and synthetic (PLGA) scaffolds (**Figure 7*a***). These nanoelectronic scaffolds (nanoES) exhibited porosities comparable to those seen for their bulk-hydrogel counterparts. Not only did these nanoES report long-term viabilities for neurons and cardiomyocytes, but they also were used to monitor the electrical activities of the cardiomyocytes. Furthermore, the authors proposed that the applications of these nanoES could be expanded to provide both electrical and mechanical stimulation for the cells. Thus, in the future, nanoES might sense the physiological activities of cells and then provide electrical and/or mechanical stimulation to enhance the cells' growth and proliferation.

Recently, the Khademhosseini group (169) incorporated carbon nanotubes (CNTs) in GelMA hydrogels. CNT-GelMA hydrodels showed enhanced viability and phenotypical characteristics of neonatal rat ventricular myocytes compared with unmodified GelMA hydrogels (**Figure 7*b***). In addition, the cardiac cells showed 3-fold greater spontaneous beating rates and an 85% lower excitation threshold. The cardiac tissues cultured in CNT-GelMA hydrogels showed less damage from cytotoxic compounds such as heptanol and doxorubicin. Finally, the authors also demonstrated both spontaneous and electrically stimulated motion of CNT-GelMA-based 2D biohybrid actuators. Next-generation scaffolds could incorporate both the sensing (168) and the actuating (169) elements together to truly mimic the physiological microenvironments experienced by cells.

In order to allow the development of thicker tissues and prevent formation of a necrotic core within a scaffold, it is very important that perfusable vascular networks allow the exchange of gases, nutrients, and metabolic products (170–172). Most of the current fabrication strategies have developed scaffolds that are capable of culturing cells only for short periods of time in relatively small constructs. However, both the current and next generations of biofabrication techniques need to address the challenge of fabricating a network of microvessels within a scaffold for long-term studies to allow the formation of larger and thicker tissue constructs. Recently, Miller et al. (173) printed a 3D network of carbohydrate glass as a sacrificial template within different types of hydrogels. To prevent disruption in the ECM cross-linking during dissolution, this carbohydrate glass was coated with a thin layer of poly(D-lactide-co-glycolide) (**Figure 7*c***). After dissolution of the carbohydrate glass, an interconnected open cylindrical lumen was left behind within the hydrogel. This lumen network supported the growth of human umbilical vein endothelial cells and also allowed for perfusion of liquid. Furthermore, rat hepatocytes showed improved functionality in the hydrogels with perfused vascular networks versus in bulk hydrogels. The authors also claimed that because it is independent of the bulk scaffold fabrication, the vascular casting approach could be applied to a number of other biofabrication techniques and will be compatible with different cross-linking strategies. This and other types of vascularization strategies need to be incorporated with the different biofabrication strategies to develop scaffolds that are capable of larger-tissue growth and development.

In the future, biofabrication technologies might fabricate scaffolds that will both differentiate stem cells and provide microenvironmental cues that allow the maturation of these cells into adult tissue. It would then be possible to develop organs on demand in vitro, thereby lowering or completely eliminating the need for organ donation from individuals. Given the potential applications of tissue-engineered organs, this manufacturing technology could revolutionize modern medicine and health care.

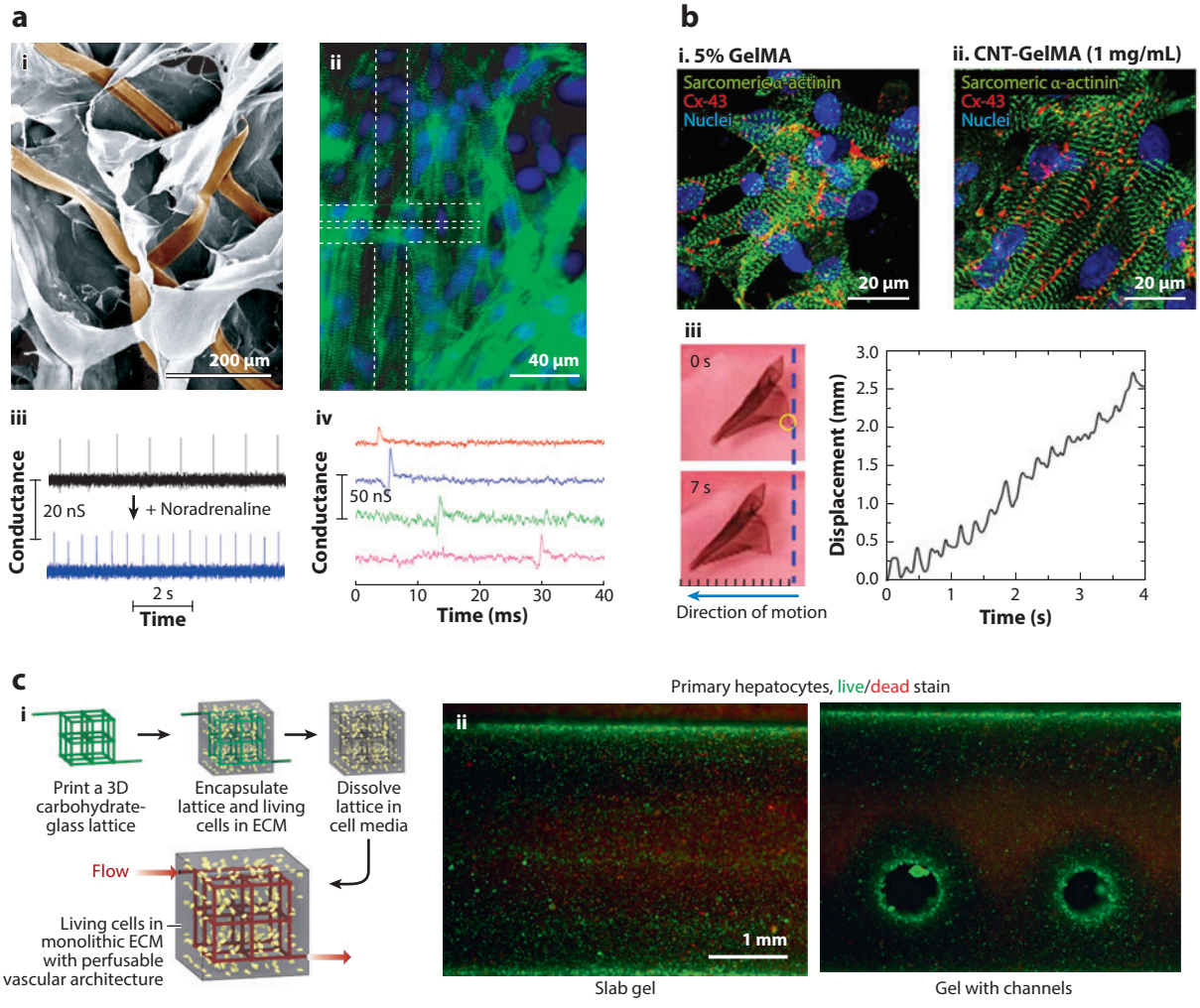

Figure 7

Next-generation biofabrication techniques. (*a*,*i*) SEM image of a nanoES made of alginate. The epoxy ribbons are false-colored brown for clarity. (*ii*) Fluorescence image of a cardiac patch. Green shows α-actin, and blue indicates cell nuclei. The dashed lines show the position of the source–drain electrodes. (*iii*) Monitoring capability (conductance versus time) of the nanoES sensor in a 3D cardiomyocyte mesh before (*black*) and after (*blue*) applying noradrenaline. (*iv*) Multiplexed simultaneous electrical recording of the extracellular field potentials from four nanowire FETs with 6.8-mm separation in a nanoES/cardiac construct (168). (*b*) Immunofluorescent images of sarcomeric α-actinin (*green*), nuclei (*blue*), and Cx-43 (*red*) on (*i*) pristine GelMA and (*ii*) CNT-GelMA. (*iii*) Spontaneous locomotion of a triangular swimmer at different time points and the corresponding displacement versus time plot (169). (*c*,*i*) Schematic overview of an open interconnected self-supporting glass lattice that serves as a sacrificial element for the casting of 3D vascular architectures. (*ii*) Primary rat hepatocytes and fibroblasts in agarose gel (slab versus channeled) after 8 days of culture stained with live/dead assay. Green indicates live cells, whereas red shows dead ones (173). Abbreviations: 3D, three-dimensional; CNT-GelMA, carbon nanotubes incorporated into GelMA; ECM, extracellular matrix; FETs, field-effect transistors; GelMA, gelatin methacrylate; nanoES, nanoelectronic scaffold. (Reprinted with permission from Nature Publishing Group and the American Chemical Society.)

DISCLOSURE STATEMENT

The authors are not aware of any affiliations, memberships, funding, or financial holdings that might be perceived as affecting the objectivity of this review.

ACKNOWLEDGMENTS

P.B. and R.B. acknowledge US Army Medical Research and Materiel Command Telemedicine & Advanced Technology Research Center (Contract No. W81XWH0810701) and National Science Foundation Science and Technology Center (Emergent Behaviors of Integrated Cellular Systems Grant CBET-0939511) for funding. Funding for R.M.S. was provided by a Ruth L. Kirschstein National Research Service Award (F32HL120650). A.K. acknowledges funding from the NIH (AR057837, AI081534, and EB02597) and the Presidential Early Career Award for Scientists and Engineers (PECASE).

LITERATURE CITED

1. US Dep. Health Hum. Serv. 2014. *The need is real: data*. Donate the Gift of Life Statistics and Figures, US Dep. Health Hum. Serv., Washington, DC, retrieved February 26, 2014. **http://www.organdonor.gov/about/data.html**
2. Langer R, Vacanti JP. 1993. Tissue engineering. *Science* 260:920–26
3. Nerem RM. 1991. Cellular engineering. *Ann. Biomed. Eng.* 19:529–45
4. Compton CC, Butler CE, Yannas IV, Warland G, Orgill DP. 1998. Organized skin structure is regenerated in vivo from collagen-GAG matrices seeded with autologous keratinocytes. *J. Investig. Dermatol.* 110:908–16
5. Vunjak-Novakovic G, Obradovic B, Martin I, Bursac PM, Langer R, Freed LE. 1998. Dynamic cell seeding of polymer scaffolds for cartilage tissue engineering. *Biotechnol. Prog.* 14:193–202
6. Jungebluth P, Alici E, Baiguera S, Le Blanc K, Blomberg P, et al. 2011. Tracheobronchial transplantation with a stem-cell-seeded bioartificial nanocomposite: a proof-of-concept study. *Lancet* 378:1997–2004
7. Atala A, Bauer SB, Soker S, Yoo JJ, Retik AB. 2006. Tissue-engineered autologous bladders for patients needing cystoplasty. *Lancet* 367:1241–46
8. Lovett M, Lee K, Edwards A, Kaplan DL. 2009. Vascularization strategies for tissue engineering. *Tissue Eng. Part B Rev.* 15:353–70
9. Huebsch N, Arany PR, Mao AS, Shvartsman D, Ali OA, et al. 2010. Harnessing traction-mediated manipulation of the cell/matrix interface to control stem-cell fate. *Nat. Mater.* 9:518–26
10. Gill BJ, Gibbons DL, Roudsari LC, Saik JE, Rizvi ZH, et al. 2012. A synthetic matrix with independently tunable biochemistry and mechanical properties to study epithelial morphogenesis and EMT in a lung adenocarcinoma model. *Cancer Res.* 72:6013–23
11. Khetan S, Burdick JA. 2010. Patterning network structure to spatially control cellular remodeling and stem cell fate within 3-dimensional hydrogels. *Biomaterials* 31:8228–34
12. Naito H, Yoshimura M, Mizuno T, Takasawa S, Tojo T, Taniguchi S. 2013. The advantages of three-dimensional culture in a collagen hydrogel for stem cell differentiation. *J. Biomed. Mater. Res. A* 101:2838–45
13. Baker BM, Chen CS. 2012. Deconstructing the third dimension: how 3D culture microenvironments alter cellular cues. *J. Cell Sci.* 125:3015–24
14. Pataky K, Braschler T, Negro A, Renaud P, Lutolf MP, Brugger J. 2012. Microdrop printing of hydrogel bioinks into 3D tissue-like geometries. *Adv. Mater.* 24:391–96
15. Culver JC, Hoffmann JC, Poche RA, Slater JH, West JL, Dickinson ME. 2012. Three-dimensional biomimetic patterning in hydrogels to guide cellular organization. *Adv. Mater.* 24:2344–48
16. Edalat F, Sheu I, Manoucheri S, Khademhosseini A. 2012. Material strategies for creating artificial cell-instructive niches. *Curr. Opin. Biotechnol.* 23:820–25

17. Buchanan CF, Voigt EE, Szot CS, Freeman JW, Vlachos PP, Rylander MN. 2014. Three-dimensional microfluidic collagen hydrogels for investigating flow-mediated tumor-endothelial signaling and vascular organization. *Tissue Eng. Part C Methods* 20:64–75
18. Zhang L, Yuan T, Guo L, Zhang X. 2012. An in vitro study of collagen hydrogel to induce the chondrogenic differentiation of mesenchymal stem cells. *J. Biomed. Mater. Res. A* 100:2717–25
19. Zhang X, Xu L, Huang X, Wei S, Zhai M. 2012. Structural study and preliminary biological evaluation on the collagen hydrogel crosslinked by γ-irradiation. *J. Biomed. Mater. Res. A* 100:2960–69
20. Hwang CM, Ay B, Kaplan DL, Rubin JP, Marra KG, et al. 2013. Assessments of injectable alginate particle-embedded fibrin hydrogels for soft tissue reconstruction. *Biomed. Mater.* 8:014105
21. McCall AD, Nelson JW, Leigh NJ, Duffey ME, Lei P, et al. 2013. Growth factors polymerized within fibrin hydrogel promote amylase production in parotid cells. *Tissue Eng. Part A* 19:2215–25
22. Thomson KS, Korte FS, Giachelli CM, Ratner BD, Regnier M, Scatena M. 2013. Prevascularized microtemplated fibrin scaffolds for cardiac tissue engineering applications. *Tissue Eng. Part A* 19:967–77
23. Burdick JA, Chung C, Jia X, Randolph MA, Langer R. 2005. Controlled degradation and mechanical behavior of photopolymerized hyaluronic acid networks. *Biomacromolecules* 6:386–91
24. Burdick JA, Prestwich GD. 2011. Hyaluronic acid hydrogels for biomedical applications. *Adv. Mater.* 23:H41–56
25. Liu Y, Charles LF, Zarembinski TI, Johnson KI, Atzet SK, et al. 2012. Modified hyaluronan hydrogels support the maintenance of mouse embryonic stem cells and human induced pluripotent stem cells. *Macromol. Biosci.* 12:1034–42
26. Suri S, Schmidt CE. 2009. Photopatterned collagen-hyaluronic acid interpenetrating polymer network hydrogels. *Acta Biomater.* 5:2385–97
27. Jin L, Feng T, Shih HP, Zerda R, Luo A, et al. 2013. Colony-forming cells in the adult mouse pancreas are expandable in Matrigel and form endocrine/acinar colonies in laminin hydrogel. *Proc. Natl. Acad. Sci. USA* 110:3907–12
28. Schumann P, Lindhorst D, Von See C, Menzel N, Kampmann A, et al. 2014. Accelerating the early angiogenesis of tissue engineering constructs in vivo by the use of stem cells cultured in Matrigel. *J. Biomed. Mater. Res. A* 102:1652–62
29. Sodunke TR, Turner KK, Caldwell SA, McBride KW, Reginato MJ, Noh HM. 2007. Micropatterns of Matrigel for three-dimensional epithelial cultures. *Biomaterials* 28:4006–16
30. Aizawa Y, Wylie R, Shoichet M. 2010. Endothelial cell guidance in 3D patterned scaffolds. *Adv. Mater.* 22:4831–35
31. Luo Y, Shoichet MS. 2004. A photolabile hydrogel for guided three-dimensional cell growth and migration. *Nat. Mater.* 3:249–53
32. Hughes CS, Postovit LM, Lajoie GA. 2010. Matrigel: a complex protein mixture required for optimal growth of cell culture. *Proteomics* 10:1886–90
33. Guvendiren M, Burdick JA. 2010. The control of stem cell morphology and differentiation by hydrogel surface wrinkles. *Biomaterials* 31:6511–18
34. Hanson Shepherd JN, Parker ST, Shepherd RF, Gillette MU, Lewis JA, Nuzzo RG. 2011. 3D microperiodic hydrogel scaffolds for robust neuronal cultures. *Adv. Funct. Mater.* 21:47–54
35. Barry RA, Shepherd RF, Hanson JN, Nuzzo RG, Wiltzius P, Lewis JA. 2009. Direct-write assembly of 3D hydrogel scaffolds for guided cell growth. *Adv. Mater.* 21:2407–10
36. Tekin H, Sanchez JG, Landeros C, Dubbin K, Langer R, Khademhosseini A. 2012. Controlling spatial organization of multiple cell types in defined 3D geometries. *Adv. Mater.* 24:5543–47
37. Zhu JM. 2010. Bioactive modification of poly(ethylene glycol) hydrogels for tissue engineering. *Biomaterials* 31:4639–56
38. Chan BK, Wippich CC, Wu CJ, Sivasankar PM, Schmidt G. 2012. Robust and semi-interpenetrating hydrogels from poly(ethylene glycol) and collagen for elastomeric tissue scaffolds. *Macromol. Biosci.* 12:1490–501
39. Hong Y, Huber A, Takanari K, Amoroso NJ, Hashizume R, et al. 2011. Mechanical properties and in vivo behavior of a biodegradable synthetic polymer microfiber-extracellular matrix hydrogel biohybrid scaffold. *Biomaterials* 32:3387–94

40. Sui ZJ, King WJ, Murphy WL. 2007. Dynamic materials based on a protein conformational change. *Adv. Mater.* 19:3377–80
41. Annabi N, Tsang K, Mithieux SM, Nikkhah M, Ameri A, et al. 2013. Highly elastic micropatterned hydrogel for engineering functional cardiac tissue. *Adv. Funct. Mater.* 23:4950–59
42. Rydholm AE, Anseth KS, Bowman CN. 2007. Effects of neighboring sulfides and pH on ester hydrolysis in thiol-acrylate photopolymers. *Acta Biomater.* 3:449–55
43. Martens P, Metters AT, Anseth KS, Bowman CN. 2001. A generalized bulk-degradation model for hydrogel networks formed from multivinyl cross-linking molecules. *J. Phys. Chem. B* 105:5131–38
44. Metters AT, Anseth KS, Bowman CN. 2000. Fundamental studies of a novel, biodegradable PEG-b-PLA hydrogel. *Polymer* 41:3993–4004
45. Shih H, Lin CC. 2012. Cross-linking and degradation of step-growth hydrogels formed by thiol-ene photoclick chemistry. *Biomacromolecules* 13:2003–12
46. Cho E, Kutty JK, Datar K, Lee JS, Vyavahare NR, Webb K. 2009. A novel synthetic route for the preparation of hydrolytically degradable synthetic hydrogels. *J. Biomed. Mater. Res. A* 90A:1073–82
47. Elbert DL, Pratt AB, Lutolf MP, Halstenberg S, Hubbell JA. 2001. Protein delivery from materials formed by self-selective conjugate addition reactions. *J. Control. Release* 76:11–25
48. Rydholm AE, Bowman CN, Anseth KS. 2005. Degradable thiol-acrylate photopolymers: polymerization and degradation behavior of an in situ forming biomaterial. *Biomaterials* 26:4495–506
49. Rydholm AE, Reddy SK, Anseth KS, Bowman CN. 2007. Development and characterization of degradable thiol-allyl ether photopolymers. *Polymer* 48:4589–600
50. Khetan S, Guvendiren M, Legant WR, Cohen DM, Chen CS, Burdick JA. 2013. Degradation-mediated cellular traction directs stem cell fate in covalently crosslinked three-dimensional hydrogels. *Nat. Mater.* 12:458–65
51. Miller JS, Shen CJ, Legant WR, Baranski JD, Blakely BL, Chen CS. 2010. Bioactive hydrogels made from step-growth derived PEG-peptide macromers. *Biomaterials* 31:3736–43
52. West JL, Hubbell JA. 1998. Polymeric biomaterials with degradation sites for proteases involved in cell migration. *Macromolecules* 32:241–44
53. Jo YS, Rizzi SC, Ehrbar M, Weber FE, Hubbell JA, Lutolf MP. 2010. Biomimetic PEG hydrogels crosslinked with minimal plasmin-sensitive tri-amino acid peptides. *J. Biomed. Mater. Res. A* 93:870–77
54. Halstenberg S, Panitch A, Rizzi S, Hall H, Hubbell JA. 2002. Biologically engineered protein-graft-poly(ethylene glycol) hydrogels: a cell adhesive and plasmin-degradable biosynthetic material for tissue repair. *Biomacromolecules* 3:710–23
55. Patterson J, Hubbell JA. 2010. Enhanced proteolytic degradation of molecularly engineered PEG hydrogels in response to MMP-1 and MMP-2. *Biomaterials* 31:7836–45
56. Aubin H, Nichol JW, Hutson CB, Bae H, Sieminski AL, et al. 2010. Directed 3D cell alignment and elongation in microengineered hydrogels. *Biomaterials* 31:6941–51
57. Mironov V, Prestwich G, Forgacs G. 2007. Bioprinting living structures. *J. Mater. Chem.* 17:2054–60
58. Cuchiara MP, Gould DJ, McHale MK, Dickinson ME, West JL. 2012. Integration of self-assembled microvascular networks with microfabricated peg-based hydrogels. *Adv. Funct. Mater.* 22:4511–18
59. Moon JJ, Lee SH, West JL. 2007. Synthetic biomimetic hydrogels incorporated with ephrin-A1 for therapeutic angiogenesis. *Biomacromolecules* 8:42–49
60. Killops KL, Campos LM, Hawker CJ. 2008. Robust, efficient, and orthogonal synthesis of dendrimers via thiol-ene "click" chemistry. *J. Am. Chem. Soc.* 130:5062–64
61. Polizzotti BD, Fairbanks BD, Anseth KS. 2008. Three-dimensional biochemical patterning of click-based composite hydrogels via thiolene photopolymerization. *Biomacromolecules* 9:1084–87
62. Fairbanks BD, Scott TF, Kloxin CJ, Anseth KS, Bowman CN. 2009. Thiol-yne photopolymerizations: novel mechanism, kinetics, and step-growth formation of highly cross-linked networks. *Macromolecules* 42:211–17
63. Lomba M, Oriol L, Alcala R, Sanchez C, Moros M, et al. 2011. In situ photopolymerization of biomaterials by thiol-yne click chemistry. *Macromol. Biosci.* 11:1505–14
64. Lutolf MP, Hubbell JA. 2003. Synthesis and physicochemical characterization of end-linked poly(ethylene glycol)-co-peptide hydrogels formed by Michael-type addition. *Biomacromolecules* 4:713–22

65. Seliktar D, Zisch AH, Lutolf MP, Wrana JL, Hubbell JA. 2004. MMP-2 sensitive, VEGF-bearing bioactive hydrogels for promotion of vascular healing. *J. Biomed. Mater. Res. A* 68:704–16
66. DeForest CA, Anseth KS. 2011. Cytocompatible click-based hydrogels with dynamically tunable properties through orthogonal photoconjugation and photocleavage reactions. *Nat. Chem.* 3:925–31
67. DeForest CA, Anseth KS. 2012. Photoreversible patterning of biomolecules within click-based hydrogels. *Angew. Chem. Int. Ed.* 51:1816–19
68. DeForest CA, Polizzotti BD, Anseth KS. 2009. Sequential click reactions for synthesizing and patterning three-dimensional cell microenvironments. *Nat. Mater.* 8:659–64
69. Deforest CA, Sims EA, Anseth KS. 2010. Peptide-functionalized click hydrogels with independently tunable mechanics and chemical functionality for 3D cell culture. *Chem. Mater.* 22:4783–90
70. Annabi N, Nichol JW, Zhong X, Ji C, Koshy S, et al. 2010. Controlling the porosity and microarchitecture of hydrogels for tissue engineering. *Tissue Eng. Part B Rev.* 16:371–83
71. Mikos AG, Thorsen AJ, Czerwonka LA, Bao Y, Langer R, et al. 1994. Preparation and characterization of poly(l-lactic acid) foams. *Polymer* 35:1068–77
72. Mehrabanian M, Nasr-Esfahani M. 2011. HA/nylon 6,6 porous scaffolds fabricated by salt-leaching/solvent casting technique: effect of nano-sized filler content on scaffold properties. *Int. J. Nanomed.* 6:1651–59
73. Park JS, Woo DG, Sun BK, Chung H-M, Im SJ, et al. 2007. In vitro and in vivo test of PEG/PCL-based hydrogel scaffold for cell delivery application. *J. Control. Release* 124:51–59
74. Ford MC, Bertram JP, Hynes SR, Michaud M, Li Q, et al. 2006. A macroporous hydrogel for the coculture of neural progenitor and endothelial cells to form functional vascular networks in vivo. *Proc. Natl. Acad. Sci. USA* 103:2512–17
75. Madihally SV, Matthew HWT. 1999. Porous chitosan scaffolds for tissue engineering. *Biomaterials* 20:1133–42
76. Hsu Y-Y, Gresser JD, Trantolo DJ, Lyons CM, Gangadharam PRJ, Wise DL. 1997. Effect of polymer foam morphology and density on kinetics of in vitro controlled release of isoniazid from compressed foam matrices. *J. Biomed. Mater. Res.* 35:107–16
77. Kang H-W, Tabata Y, Ikada Y. 1999. Effect of porous structure on the degradation of freeze-dried gelatin hydrogels. *J. Bioact. Compat. Polym.* 14:331–43
78. Kang H-W, Tabata Y, Ikada Y. 1999. Fabrication of porous gelatin scaffolds for tissue engineering. *Biomaterials* 20:1339–44
79. Shapiro L, Cohen S. 1997. Novel alginate sponges for cell culture and transplantation. *Biomaterials* 18:583–90
80. Miyata T, Sohde T, Rubin AL, Stenzel KH. 1971. Effects of ultraviolet irradiation on native and telopeptide-poor collagen. *Biochim. Biophys. Acta* 229:672–80
81. Peng Z, Chen F. 2010. Hydroxyethyl cellulose-based hydrogels with various pore sizes prepared by freeze-drying. *J. Macromol. Sci. Part B Phys.* 50:340–49
82. Lai J-Y, Ma DH-K, Lai M-H, Li Y-T, Chang R-J, Chen L-M. 2013. Characterization of cross-linked porous gelatin carriers and their interaction with corneal endothelium: biopolymer concentration effect. *PLoS ONE* 8:e54058
83. Ho M-H, Kuo P-Y, Hsieh H-J, Hsien T-Y, Hou L-T, et al. 2004. Preparation of porous scaffolds by using freeze-extraction and freeze-gelation methods. *Biomaterials* 25:129–38
84. Quirk RA, France RM, Shakesheff KM, Howdle SM. 2004. Supercritical fluid technologies and tissue engineering scaffolds. *Curr. Opin. Solid State Mater. Sci.* 8:313–21
85. Zellander A, Gemeinhart R, Djalilian A, Makhsous M, Sun S, Cho M. 2013. Designing a gas foamed scaffold for keratoprosthesis. *Mater. Sci. Eng. C Mater. Biol. Appl.* 33:3396–403
86. Haugen H, Reid V, Brunner M, Will J, Wintermantel E. 2004. Water as a foaming agent for open cell polyurethane structures. *J. Mater. Sci.: Mater. Med.* 15:343–46
87. Mooney DJ, Baldwin DF, Suh NP, Vacanti JP, Langer R. 1996. Novel approach to fabricate porous sponges of poly(D,L-lactic-co-glycolic acid) without the use of organic solvents. *Biomaterials* 17:1417–22
88. Sachlos E, Czernuszka JT. 2003. Making tissue engineering scaffolds work. Review: The application of solid freeform fabrication technology to the production of tissue engineering scaffolds. *Eur. Cells Mater.* 5:29–40

89. Harris LD, Kim BS, Mooney DJ. 1998. Open pore biodegradable matrices formed with gas foaming. *J. Biomed. Mater. Res.* 42:396–402
90. Kim H, Park I, Kim J, Cho C, Kim M. 2012. Gas foaming fabrication of porous biphasic calcium phosphate for bone regeneration. *Tissue Eng. Regen. Med.* 9:63–68
91. Nam YS, Yoon JJ, Park TG. 2000. A novel fabrication method of macroporous biodegradable polymer scaffolds using gas foaming salt as a porogen additive. *J. Biomed. Mater. Res.* 53:1–7
92. Mironov V, Visconti RP, Kasyanov V, Forgacs G, Drake CJ, Markwald RR. 2009. Organ printing: tissue spheroids as building blocks. *Biomaterials* 30:2164–74
93. Norotte C, Marga FS, Niklason LE, Forgacs G. 2009. Scaffold-free vascular tissue engineering using bioprinting. *Biomaterials* 30:5910–17
94. Boland T, Xu T, Damon B, Cui X. 2006. Application of inkjet printing to tissue engineering. *Biotechnol. J.* 1:910–17
95. Xu T, Jin J, Gregory C, Hickman JJ, Boland T. 2005. Inkjet printing of viable mammalian cells. *Biomaterials* 26:93–99
96. Cui XF, Boland T. 2009. Human microvasculature fabrication using thermal inkjet printing technology. *Biomaterials* 30:6221–27
97. Villar G, Graham AD, Bayley H. 2013. A tissue-like printed material. *Science* 340:48–52
98. Lewis JA. 2006. Direct ink writing of 3D functional materials. *Adv. Funct. Mater.* 16:2193–204
99. Smay JE, Gratson GM, Shepherd RF, Cesarano J, Lewis JA. 2002. Directed colloidal assembly of 3D periodic structures. *Adv. Mater.* 14:1279–83
100. Duoss EB, Twardowski M, Lewis JA. 2007. Sol-gel inks for direct-write assembly of functional oxides. *Adv. Mater.* 19:3485–89
101. Sun J, Tang J, Ding J. 2009. Cell orientation on a stripe-micropatterned surface. *Chin. Sci. Bull.* 54:3154–59
102. Lee S-H, Moon JJ, West JL. 2008. Three-dimensional micropatterning of bioactive hydrogels via two-photon laser scanning photolithography for guided 3D cell migration. *Biomaterials* 29:2962–68
103. Williams CG, Malik AN, Kim TK, Manson PN, Elisseeff JH. 2005. Variable cytocompatibility of six cell lines with photoinitiators used for polymerizing hydrogels and cell encapsulation. *Biomaterials* 26:1211–18
104. Liu Tsang V, Chen AA, Cho LM, Jadin KD, Sah RL, et al. 2007. Fabrication of 3D hepatic tissues by additive photopatterning of cellular hydrogels. *FASEB J.* 21:790–801
105. Hahn MS, Miller JS, West JL. 2006. Three-dimensional biochemical and biomechanical patterning of hydrogels for guiding cell behavior. *Adv. Mater.* 18:2679–84
106. Bajaj P, Marchwiany D, Duarte C, Bashir R. 2013. Patterned three-dimensional encapsulation of embryonic stem cells using dielectrophoresis and stereolithography. *Adv. Healthc. Mater.* 2:450–58
107. Zorlutuna P, Jeong JH, Kong H, Bashir R. 2011. Stereolithography-based hydrogel microenvironments to examine cellular interactions. *Adv. Funct. Mater.* 21:3642–51
108. Bryant SJ, Nuttelman CR, Anseth KS. 2000. Cytocompatibility of UV and visible light photoinitiating systems on cultured NIH/3T3 fibroblasts in vitro. *J. Biomater. Sci. Polym. Ed.* 11:439–57
109. Miller GA, Gou L, Narayanan V, Scranton AB. 2002. Modeling of photobleaching for the photoinitiation of thick polymerization systems. *J. Polym. Sci. Part A Polym. Chem.* 40:793–808
110. Terrones G, Pearlstein AJ. 2001. Effects of kinetics and optical attenuation on the completeness, uniformity, and dynamics of monomer conversion in free-radical photopolymerizations. *Macromolecules* 34:8894–906
111. Ivanov VV, Decker C. 2001. Kinetic study of photoinitiated frontal polymerization. *Polym. Int.* 50:113–18
112. Fukuda J, Khademhosseini A, Yeo Y, Yang X, Yeh J, et al. 2006. Micromolding of photocrosslinkable chitosan hydrogel for spheroid microarray and co-cultures. *Biomaterials* 27:5259–67
113. Khademhosseini A, Eng G, Yeh J, Fukuda J, Blumling J, et al. 2006. Micromolding of photocrosslinkable hyaluronic acid for cell encapsulation and entrapment. *J. Biomed. Mater. Res. A* 79A:522–32
114. Liu VA, Bhatia SN. 2002. Three-dimensional photopatterning of hydrogels containing living cells. *Biomed. Microdevices* 4:257–66
115. Yeh J, Ling Y, Karp JM, Gantz J, Chandawarkar A, et al. 2006. Micromolding of shape-controlled, harvestable cell-laden hydrogels. *Biomaterials* 27:5391–98

116. Bajaj P, Tang X, Saif TA, Bashir R. 2010. Stiffness of the substrate influences the phenotype of embryonic chicken cardiac myocytes. *J. Biomed. Mater. Res. A* 95A:1261–69
117. Discher DE, Janmey P, Wang Y-l. 2005. Tissue cells feel and respond to the stiffness of their substrate. *Science* 310:1139–43
118. Bajaj P, Reddy B, Millet L, Wei C, Zorlutuna P, et al. 2011. Patterning the differentiation of C2C12 skeletal myoblasts. *Integr. Biol.* 3:897–909
119. McBeath R, Pirone DM, Nelson CM, Bhadriraju K, Chen CS. 2004. Cell shape, cytoskeletal tension, and RhoA regulate stem cell lineage commitment. *Dev. Cell* 6:483–95
120. Ghibaudo M, Trichet L, Le Digabel J, Richert A, Hersen P, Ladoux B. 2009. Substrate topography induces a crossover from 2D to 3D behavior in fibroblast migration. *Biophys. J.* 97:357–68
121. Chen W, Villa-Diaz LG, Sun Y, Weng S, Kim JK, et al. 2012. Nanotopography influences adhesion, spreading, and self-renewal of human embryonic stem cells. *ACS Nano* 6:4094–103
122. Kim D-H, Provenzano PP, Smith CL, Levchenko A. 2012. Matrix nanotopography as a regulator of cell function. *J. Cell Biol.* 197:351–60
123. Bajaj P, Khang D, Webster TJ. 2006. Control of spatial cell attachment on carbon nanofiber patterns on polycarbonate urethane. *Int. J. Nanomed.* 1:361–65
124. Deligianni DD, Katsala ND, Koutsoukos PG, Missirlis YF. 2000. Effect of surface roughness of hydroxyapatite on human bone marrow cell adhesion, proliferation, differentiation and detachment strength. *Biomaterials* 22:87–96
125. Dowling DP, Miller IS, Ardhaoui M, Gallagher WM. 2011. Effect of surface wettability and topography on the adhesion of osteosarcoma cells on plasma-modified polystyrene. *J. Biomater. Appl.* 26:327–47
126. Lampin M, Warocquier-Clérout R, Legris C, Degrange M, Sigot-Luizard MF. 1997. Correlation between substratum roughness and wettability, cell adhesion, and cell migration. *J. Biomed. Mater. Res.* 36:99–108
127. Ross AM, Jiang Z, Bastmeyer M, Lahann J. 2012. Physical aspects of cell culture substrates: topography, roughness, and elasticity. *Small* 8:336–55
128. Ward M, Dembo M, Hammer D. 1995. Kinetics of cell detachment: effect of ligand density. *Ann. Biomed. Eng.* 23:322–31
129. Zheng X, Cheung LS-L, Schroeder JA, Jiang L, Zohar Y. 2011. Cell receptor and surface ligand density effects on dynamic states of adhering circulating tumor cells. *Lab Chip* 11:3431–39
130. Marklein RA, Burdick JA. 2010. Spatially controlled hydrogel mechanics to modulate stem cell interactions. *Soft Matter* 6:136–43
131. Burdick JA, Khademhosseini A, Langer R. 2004. Fabrication of gradient hydrogels using a microfluidics/photopolymerization process. *Langmuir* 20:5153–56
132. Lanniel M, Huq E, Allen S, Buttery L, Williams PM, Alexander MR. 2011. Substrate induced differentiation of human mesenchymal stem cells on hydrogels with modified surface chemistry and controlled modulus. *Soft Matter* 7:6501–14
133. Nichol JW, Koshy ST, Bae H, Hwang CM, Yamanlar S, Khademhosseini A. 2010. Cell-laden microengineered gelatin methacrylate hydrogels. *Biomaterials* 31:5536–44
134. Engler AJ, Sen S, Sweeney HL, Discher DE. 2006. Matrix elasticity directs stem cell lineage specification. *Cell* 126:677–89
135. Occhetta P, Sadr N, Piraino F, Redaelli A, Moretti M, Rasponi M. 2013. Fabrication of 3D cell-laden hydrogel microstructures through photo-mold patterning. *Biofabrication* 5:1–10
136. Bryant SJ, Cuy JL, Hauch KD, Ratner BD. 2007. Photo-patterning of porous hydrogels for tissue engineering. *Biomaterials* 28:2978–86
137. Hammoudi TM, Lu H, Temenoff JS. 2010. Long-term spatially defined coculture within three-dimensional photopatterned hydrogels. *Tissue Eng. Part C Methods* 16:1621–28
138. Melchels FPW, Feijen J, Grijpma DW. 2010. A review on stereolithography and its applications in biomedical engineering. *Biomaterials* 31:6121–30
139. Lantada AD, Morgado PL. 2012. Rapid prototyping for biomedical engineering: current capabilities and challenges. *Annu. Rev. Biomed. Eng.* 14:73–96

140. Bajaj P, Chan V, Jae Hyun J, Zorlutuna P, Hyunjoon K, Bashir R. 2012. 3-D biofabrication using stereolithography for biology and medicine. *Conf. Proc. Eng. Med. Biol. Soc. (EMBC), Annu. Int. Conf. IEEE, San Diego*, pp. 6805–8. New York: IEEE
141. Dhariwala B, Hunt E, Boland T. 2004. Rapid prototyping of tissue-engineering constructs, using photopolymerizable hydrogels and stereolithography. *Tissue Eng.* 10:1316–22
142. Arcaute K, Mann BK, Wicker RB. 2006. Stereolithography of three-dimensional bioactive poly(ethylene glycol) constructs with encapsulated cells. *Ann. Biomed. Eng.* 34:1429–41
143. Chan V, Zorlutuna P, Jeong JH, Kong H, Bashir R. 2010. Three-dimensional photopatterning of hydrogels using stereolithography for long-term cell encapsulation. *Lab Chip* 10:2062–70
144. Seck TM, Melchels FPW, Feijen J, Grijpma DW. 2010. Designed biodegradable hydrogel structures prepared by stereolithography using poly(ethylene glycol)/poly(d,l-lactide)-based resins. *J. Control. Release* 148:34–41
145. Jeong JH, Chan V, Cha C, Zorlutuna P, Dyck C, et al. 2012. "Living" microvascular stamp for patterning of functional neovessels; orchestrated control of matrix property and geometry. *Adv. Mater.* 24:58–63
146. Melchels FPW, Feijen J, Grijpma DW. 2009. A poly(d,l-lactide) resin for the preparation of tissue engineering scaffolds by stereolithography. *Biomaterials* 30:3801–9
147. Lee S-J, Kang H-W, Park J, Rhie J-W, Hahn S, Cho D-W. 2008. Application of microstereolithography in the development of three-dimensional cartilage regeneration scaffolds. *Biomed. Microdevices* 10:233–41
148. Leigh SJ, Gilbert HTJ, Barker IA, Becker JM, Richardson SM, et al. 2012. Fabrication of 3-dimensional cellular constructs via microstereolithography using a simple, three-component, poly(ethylene glycol) acrylate-based system. *Biomacromolecules* 14:186–92
149. Zhang AP, Qu X, Soman P, Hribar KC, Lee JW, et al. 2012. Rapid fabrication of complex 3D extracellular microenvironments by dynamic optical projection stereolithography. *Adv. Mater.* 24:4266–70
150. Maruo S, Ikuta K. 2002. Submicron stereolithography for the production of freely movable mechanisms by using single-photon polymerization. *Sens. Actuators A Phys.* 100:70–76
151. Chan V, Park K, Collens MB, Kong H, Saif TA, Bashir R. 2012. Development of miniaturized walking biological machines. *Sci. Rep.* 2:857
152. Musoke-Zawedde P, Shoichet MS. 2006. Anisotropic three-dimensional peptide channels guide neurite outgrowth within a biodegradable hydrogel matrix. *Biomed. Mater.* 1:162–69
153. Denk W, Strickler JH, Webb WW. 1990. Two-photon laser scanning fluorescence microscopy. *Science* 248:73–76
154. Zipfel WR, Williams RM, Webb WW. 2003. Nonlinear magic: multiphoton microscopy in the biosciences. *Nat. Biotechnol.* 21:1369–77
155. Hoffmann JC, West JL. 2010. Three-dimensional photolithographic patterning of multiple bioactive ligands in poly(ethylene glycol) hydrogels. *Soft Matter* 6:5056–63
156. Wosnick JH, Shoichet MS. 2008. Three-dimensional chemical patterning of transparent hydrogels. *Chem. Mater.* 20:55–60
157. Wylie RG, Shoichet MS. 2008. Two-photon micropatterning of amines within an agarose hydrogel. *J. Mater. Chem.* 18:2716–21
158. Wylie RG, Shoichet MS. 2011. Three-dimensional spatial patterning of proteins in hydrogels. *Biomacromolecules* 12:3789–96
159. Wylie RG, Ahsan S, Aizawa Y, Maxwell KL, Morshead CM, Shoichet MS. 2011. Spatially controlled simultaneous patterning of multiple growth factors in three-dimensional hydrogels. *Nat. Mater.* 10:799–806
160. Kloxin AM, Kasko AM, Salinas CN, Anseth KS. 2009. Photodegradable hydrogels for dynamic tuning of physical and chemical properties. *Science* 324:59–63
161. Kaehr B, Allen R, Javier DJ, Currie J, Shear JB. 2004. Guiding neuronal development with in situ microfabrication. *Proc. Natl. Acad. Sci. USA* 101:16104–8
162. Spikes JD, Shen HR, Kopeckova P, Kopecek J. 1999. Photodynamic crosslinking of proteins. III. Kinetics of the FMN- and rose bengal-sensitized photooxidation and intermolecular crosslinking of model tyrosine-containing N-(2-hydroxypropyl)methacrylamide copolymers. *Photochem. Photobiol.* 70:130–37
163. Seidlits SK, Schmidt CE, Shear JB. 2009. High-resolution patterning of hydrogels in three dimensions using direct-write photofabrication for cell guidance. *Adv. Funct. Mater.* 19:3543–51

164. Dankerl M, Hauf MV, Lippert A, Hess LH, Birner S, et al. 2010. Graphene solution-gated field-effect transistor array for sensing applications. *Adv. Funct. Mater.* 20:3117–24
165. Hess LH, Jansen M, Maybeck V, Hauf MV, Seifert M, et al. 2011. Graphene transistor arrays for recording action potentials from electrogenic cells. *Adv. Mater.* 23:5045–49
166. Viventi J, Kim D-H, Moss JD, Kim Y-S, Blanco JA, et al. 2010. A conformal, bio-interfaced class of silicon electronics for mapping cardiac electrophysiology. *Sci. Transl. Med.* 2:24ra22
167. Timko BP, Cohen-Karni T, Yu G, Qing Q, Tian B, Lieber CM. 2009. Electrical recording from hearts with flexible nanowire device arrays. *Nano Lett.* 9:914–18
168. Tian B, Liu J, Dvir T, Jin L, Tsui JH, et al. 2012. Macroporous nanowire nanoelectronic scaffolds for synthetic tissues. *Nat. Mater.* 11:986–94
169. Shin SR, Jung SM, Zalabany M, Kim K, Zorlutuna P, et al. 2013. Carbon-nanotube-embedded hydrogel sheets for engineering cardiac constructs and bioactuators. *ACS Nano* 7:2369–80
170. Novosel EC, Kleinhans C, Kluger PJ. 2011. Vascularization is the key challenge in tissue engineering. *Adv. Drug Deliv. Rev.* 63:300–11
171. Neumann T, Nicholson BS, Sanders JE. 2003. Tissue engineering of perfused microvessels. *Microvasc. Res.* 66:59–67
172. He J, Mao M, Liu Y, Shao J, Jin Z, Li D. 2013. Fabrication of nature-inspired microfluidic network for perfusable tissue constructs. *Adv. Healthc. Mater.* 2:1108–13
173. Miller JS, Stevens KR, Yang MT, Baker BM, Nguyen DH, et al. 2012. Rapid casting of patterned vascular networks for perfusable engineered three-dimensional tissues. *Nat. Mater.* 11:768–74

Annual Review of Biomedical Engineering
Volume 16, 2014

Contents

Indexes

Errata

An online log of corrections to *Annual Review of Biomedical Engineering* articles may be found at http://bioeng.annualreviews.org/